

DOUBLE-LOOP RANDOMIZED QUASI-MONTE CARLO ESTIMATOR FOR NESTED INTEGRATION

ARVED BARTUSKA^{#,1}, ANDRÉ GUSTAVO CARLON¹, LUIS ESPATH³, SEBASTIAN KRUMSCHEID⁵, & RAÚL TEMPONE^{1,2,4}

ABSTRACT. Nested integration of the form $\int f(\int g(\mathbf{y}, \mathbf{x}) d\mathbf{x}) d\mathbf{y}$, characterized by an outer integral connected to an inner integral through a nonlinear function f , is a challenging problem in various fields, such as engineering and mathematical finance. The available numerical methods for nested integration based on Monte Carlo (MC) methods can be prohibitively expensive owing to the error propagating from the inner to the outer integral. Attempts to enhance the efficiency of these approximations using the quasi-MC (QMC) or randomized QMC (rQMC) method have focused on either the inner or outer integral approximation. This work introduces a novel nested rQMC method that simultaneously addresses the approximation of the inner and outer integrals. The method leverages the unique nested integral structure to offer a more efficient approximation mechanism. Incorporating Owen's scrambling techniques, we address integrands exhibiting infinite variation in the Hardy–Krause sense, enabling theoretically sound error estimates. As the primary contribution, we derive asymptotic error bounds for the bias and variance of our estimator, along with the regularity conditions under which these bounds can be attained. Moreover, we derive a truncation scheme for applications in the context of expected information gain estimation and indicate how to use importance sampling to remedy the measure concentration arising in the inner integral. We verify the estimator quality through numerical experiments by comparing the computational efficiency of the nested rQMC method against standard nested MC estimation for two case studies: one in thermomechanics and the other in pharmacokinetics. These examples highlight the computational savings and enhanced applicability of the proposed approach.

Keywords: Nested integration · randomized quasi-Monte Carlo · expected information gain

AMS subject classifications: · 62F15 · 65C05 · 65D30 · 65D32 ·

ACKNOWLEDGMENTS

This publication is based upon work supported by the King Abdullah University of Science and Technology (KAUST) Office of Sponsored Research (OSR) under Award No. OSR-2019-CRG8-4033, the Alexander von Humboldt Foundation, the Deutsche Forschungsgemeinschaft (DFG, German Research Foundation) – 333849990/GRK2379 (IRTG Hierarchical and Hybrid Approaches in Modern Inverse Problems), and was partially supported by the Flexible Interdisciplinary Research Collaboration Fund at the University of Nottingham Project ID 7466664. The authors thank Yang Liu and Prof. Fabio Nobile for their helpful and constructive comments.

CONTENTS

Acknowledgments	1
1. Introduction	2
2. Brief overview of Monte Carlo and randomized quasi-Monte Carlo integration	4
2.1. Monte Carlo method	4

¹DEPARTMENT OF MATHEMATICS, RWTH AACHEN UNIVERSITY, GEBÄUDE-1953 1.OG, PONTDRIESCH 14-16, 161, 52062 AACHEN, GERMANY

²KING ABDULLAH UNIVERSITY OF SCIENCE & TECHNOLOGY (KAUST), COMPUTER, ELECTRICAL AND MATHEMATICAL SCIENCES & ENGINEERING DIVISION (CEMSE), THUWAL 23955-6900, SAUDI ARABIA

³SCHOOL OF MATHEMATICAL SCIENCES, UNIVERSITY OF NOTTINGHAM, NOTTINGHAM, NG7 2RD, UNITED KINGDOM

⁴ALEXANDER VON HUMBOLDT PROFESSOR IN MATHEMATICS FOR UNCERTAINTY QUANTIFICATION, RWTH AACHEN UNIVERSITY, GERMANY

⁵SCIENTIFIC COMPUTING CENTER, AND INSTITUTE FOR APPLIED AND NUMERICAL MATHEMATICS, KARLSRUHE INSTITUTE OF TECHNOLOGY, GERMANY

E-mail address: #arved.bartuska@gmail.com.

Date: January 16, 2025.

2.2. Quasi-Monte Carlo method	4
2.3. Randomized Quasi-Monte Carlo method	6
3. Nested integration	7
4. Numerical results	17
4.1. Example 1: Pharmacokinetics example with exact sampling	20
4.2. Example 2: Thermo-mechanics example with inexact sampling	23
5. Conclusion	29
6. Statements and Declarations	29
6.1. Conflict of interest	29
6.2. Data availability	29
Appendix A. Variance inequality	29
Appendix B. Proof of Remark 9	30
Appendix C. Verification of Assumption 1 for the EIG	30
Appendix D. Verification of Condition (42) for the EIG	34
Appendix E. Bound on the truncation error of the nested integral in the EIG	35
Appendix F. Total error of the EIG estimation via the rDLQMC estimator	38
Appendix G. Derivation of the finite element formulation	38
References	38

1. INTRODUCTION

Nested integrals are ubiquitous in numerous fields (e.g., geology [21], mathematical finance [22], medical decision-making [23], and optimal experimental design (OED) [1]). The Monte Carlo (MC) method is a commonly applied approximation technique for general integrals, especially in high dimensions. For nested integrals, both integration steps can be approximated using the MC method, resulting in the double-loop MC (DLMC) estimator [1]. To control the statistical error of an MC approximation of a single integral via the central limit theorem (CLT) [29], a sample size of $\mathcal{O}(TOL^{-2})$ is required for an error tolerance $TOL > 0$, related to an estimator's variance (to be specified later). In contrast, using DLMC to approximate nested integrals results in worse complexity, with the overall required number of samples of $\mathcal{O}(TOL^{-3})$ to achieve the same error tolerance [1]. The two MC estimators appearing in the DLMC estimator are connected through a nonlinear function; thus, the statistical error of the inner MC estimator induces bias in the DLMC estimator. The sample sizes of both MC estimators must be precisely controlled to ensure that the error in the DLMC estimator is below TOL with a certain confidence, controlling the corresponding statistical and bias errors. Improving the performance of the DLMC estimator is the goal of ongoing research, with some approaches proposing Laplace approximation [7], importance sampling [2], and multilevel MC (MLMC) methods [23].

The randomized quasi-MC (rQMC) method [24, 25, 26, 27, 30, 37] is a promising technique to improve the efficiency of the standard MC method (i.e., the required computational work to meet a tolerance) while maintaining a nonintrusive sampling structure. The rQMC estimator uses deterministic points from a low-discrepancy sequence and randomizes the entire sequence while maintaining a low-discrepancy structure. Randomization removes bias in deterministic QMC estimators, leaving only the statistical error, which can be controlled using the Chebyshev inequality or the CLT under specific conditions [28, 34, 37]. Given appropriate regularity properties of the integrand, the rQMC method can improve the order of convergence of the approximation error compared to the MC estimator. For sufficiently regular integrands, the computational work required by the rQMC estimator to achieve a tolerance TOL is $\mathcal{O}(TOL^{-1+\epsilon})$ with $\epsilon > 0$, where the multiplicative term can increase with the integrand's dimension. Owen [42] demonstrated that rQMC can yield improvements over the MC method, even for integrands with singularities at the boundaries of the integration domain (i.e., integrands with classically unfavorable regularity properties) for a randomization scheme introduced in [47]. Introducing weighted function spaces permits rQMC methods to remain competitive for high, or even infinite, dimensional integration domains under suitable regularity conditions [31]. Finally, higher-order rQMC methods enable even faster convergence at the detriment of exponential dependence on the dimension [31].

The estimation of nested integrals via MC was studied in [1] along with the theoretical error bounds in the context of the expected information gain (EIG) for OED. A more general case of a possibly discontinuous outer integrand was considered in [49], while the study [48] investigated conditions under which nested MC estimators converge. Attempts to improve upon the efficiency of MC estimators were undertaken, e.g., in [51], where the Markov chain MC method was combined with nonparametric regression for the rare event case, and in [52], where variational inference was employed to create several estimators for OED applications.

The evaluation of the integrand itself often requires an additional approximation at a specific level of accuracy. Examples of these accuracy levels include the number of time steps in temporal approximation schemes, the mesh size in finite element method (FEM) schemes, and the number of samples of inner integral estimators. A strategy for improving the effectiveness of standard MC estimators is MLMC [19], where MC estimations for integrands of various accuracy levels are combined into one highly efficient estimator. Under certain conditions, MLMC estimation can be performed without a loss of accuracy from the added approximation (i.e., at the cost of standard MC estimation, $\mathcal{O}(TOL^{-2})$). An MLMC estimator for OED was derived in [53], where the number of inner MC samples defined the levels, and [3] derived another MLMC estimator, where the number of inner MC samples and a FEM approximation defined the levels. The randomized MLMC method is an extension of the MLMC method, where the number of levels is randomized, thus removing the bias from the inner approximation. This method was applied in the context of OED in [54]; however, randomization is not always possible and places considerable restrictions on the integrands.

Recently, researchers [35] have investigated the optimal error tolerance that can be reached using rQMC, given a fixed number of samples and a specific confidence level. They demonstrated that combining rQMC with robust estimation improves error tolerance values. The rQMC concepts were applied in the context of OED in [33] but only to the outer integral of a nested integration problem. In [33], the inner integral was approximated using the MC method. For several numerical experiments, the sample standard deviation was reduced for this scheme compared to using the MC method for both integrals, which was demonstrated for a fixed number of outer and inner samples. Kaarnioja and Schillings [63] recently proposed two nested rQMC estimators for OED governed by PDEs. Based on rank-1 lattice rules with random shifts, a computational cost of $\mathcal{O}(TOL^{-2})$ is derived for their first estimator. Regularity conditions on the integrands are derived to achieve independence of the parameter dimensions. Their second estimator, moreover, employs a sparse tensor structure to achieve a computational cost of $\mathcal{O}(TOL^{-1})$. This last estimator relies on the very particular structure of the EIG. The number of samples for the outer and inner integral approximations as well as the truncation parameter for the observation noise are considered fixed, whereas in this work, we derive a near optimal setting for these quantities to maximize the efficiency of our estimator while maintaining consistency.

In recent work [23], an rQMC method was employed to approximate the outer integral of a nested estimator in medical decision-making. These authors compared this rQMC method with an MLMC approach and standard nested (i.e., double-loop) MC by specifying a target mean squared error and observing the number of samples necessary to reach the target. The interplay between rQMC and MC estimators in the nested setting was not theoretically analyzed. Both MLMC and rQMC have similar performance results in practice, depending on the number of parameters and other model complexity measures.

In [21], nested integrals were approximated using MLMC techniques. The number of inner samples was increased at each level to reduce the bias induced in the outer approximation by the variance of the inner approximation. The rQMC estimator estimated the inner integral and reduced the variance, requiring a smaller sample size in the inner loop to achieve the error tolerance in the MLMC setting in [19, Thm. 3.1]. This outcome was presented theoretically and via examples. A similar approach was followed in [22], in which a discontinuous inner integrand was approximated using a sigmoid (i.e., a smooth function), improving the performance of the rQMC method. The methods presented in [21] and [22] can achieve an error tolerance TOL at a computational cost of $\mathcal{O}(TOL^{-2})$.

This work applies the rQMC method to both integrals to build a double-loop rQMC (rDLQMC) estimator, reducing the number of samples necessary to estimate the nested integrals up to a specific error tolerance TOL at a cost close to $\mathcal{O}(TOL^{-3/2})$. Moreover, we derive sufficient regularity conditions for both the outer and inner integrands and demonstrate the advantage of replacing either of the MC approximation with rQMC approximations. We also consider the case in which the inner integrand is only approximately provided in terms of a FEM discretization, resulting in additional bias in the outer approximation. We

provide approximate error bounds for the bias and statistical error of the proposed estimator and derive a nearly optimal setting, verified via numerical examples from Bayesian OED. To make the derived error bounds applicable in this context, we verify the previously derived conditions for a simple EIG setting with truncated observation noise. The additional error introduced by this truncation is shown to affect the total error only by an insignificant contribution.

This work is structured as follows. Section 2 provides a brief overview of the MC and rQMC methods, including bounds on the L^1 and L^2 errors via the Koksma–Hlawka inequality [38, 26] and more elaborate error bounds proposed in [42] and later generalized in [45]. The subsequent Section 3 introduces the proposed novel nested rQMC estimator. As the main contributions of this work, asymptotic error bounds on the number of inner and outer samples are derived in Propositions 3 and 4 along with conditions under which these rates can be attained. Based on these bounds, the nearly optimal setting for the rDLQMC estimator is derived in Proposition 5. Finally, Section 4 presents two Bayesian OED examples where nested integrals frequently arise. The superior performance of the proposed estimators compared to other estimators is observed numerically in accordance with our theoretical results. The precise conditions derived in Section 3 are verified for a general EIG setting in Lemma 1 and 2. However, verifying the Assumptions on the particular experiment model derived in Appendix C and D is not the subject of this work to maintain generality. In Lemma 3, we bound the truncation error introduced in Appendix D, and in Corollary 1, we present the total error of the EIG estimation for our estimator. The first example aims to replicate the results in [53] for an application in pharmacokinetics to demonstrate the competitiveness and accuracy of the proposed estimator. The second example explores an application from solid mechanics involving the solution to a partial differential equation (PDE) with favorable regularity properties, demonstrating the practical applicability of the rDLQMC estimator.

2. BRIEF OVERVIEW OF MONTE CARLO AND RANDOMIZED QUASI-MONTE CARLO INTEGRATION

Before addressing the nested integration case, which is the focus of this work, we discuss the basic concepts for approximating integrals using MC, QMC, and rQMC for the reader’s convenience.

2.1. Monte Carlo method. We let $\varphi : [0, 1]^d \rightarrow \mathbb{R}$, where d is a positive integer, be square integrable. Then, the integral

$$(1) \quad I = \int_{[0,1]^d} \varphi(\mathbf{x}) \, d\mathbf{x},$$

can be approximated using the MC estimator as follows:

$$(2) \quad I_{\text{MC}} := \frac{1}{M} \sum_{m=1}^M \varphi(\mathbf{x}^{(m)}).$$

The MC method uses random points $\mathbf{x}^{(1)}, \dots, \mathbf{x}^{(M)}$, which are independent and identically distributed (iid) samples from the uniform distribution $\mathcal{U}([0, 1]^d)$, to approximate I in (1). Using the CLT to analyze the error of the MC estimator reveals that

$$(3) \quad \mathbb{P} \left(|I - I_{\text{MC}}| \leq \frac{C_\alpha \sqrt{\mathbb{V}[\varphi]}}{\sqrt{M}} \right) \geq 1 - \alpha,$$

as $M \rightarrow \infty$. Here, $\alpha \in (0, 1)$ is a parameter, $C_\alpha = \Phi^{-1}(1 - \alpha/2)$, Φ^{-1} denotes the inverse cumulative distribution function (CDF) of the standard normal distribution, and $\mathbb{V}[g]$ represents the variance of the integrand. Alternatively, Chebyshev’s inequality could be applied to obtain an error estimate similar to (3), although with a larger constant $C_\alpha = 1/\sqrt{\alpha}$.

2.2. Quasi-Monte Carlo method. The MC method converges with probability one to the true value of the integral by the strong law of large numbers, but the rate of $M^{-(1/2)}$ can be improved for certain integrands [24]. We can employ the QMC method, which achieves a better convergence rate by using specific points to exploit the regularity properties of the integrand. The QMC estimator to approximate the integral (1) is given by

$$(4) \quad I_{\text{Q}} := \frac{1}{M} \sum_{m=1}^M \varphi(\mathbf{t}^{(m)}),$$

where $\mathbf{t}^{(1)}, \dots, \mathbf{t}^{(M)} \in [0, 1]^d$ are selected from a deterministic sequence of points with low discrepancy, [26, 25]. To analyze the error of this estimator, we introduce two useful concepts. The star discrepancy [24, Def. (5.2)], defined as

$$(5) \quad D^*(\mathbf{t}^{(1)}, \dots, \mathbf{t}^{(M)}) := \sup_{(s_1, \dots, s_d) \in [0, 1]^d} \left| \frac{1}{M} \sum_{m=1}^M \mathbb{1}_{\{\mathbf{t}^{(m)} \in \prod_{i=1}^d [0, s_i]\}} - \prod_{i=1}^d s_i \right|,$$

indicates how evenly the points $\mathbf{t}^{(1)}, \dots, \mathbf{t}^{(M)}$ are distributed in $[0, 1]^d$. This concept is independent of the particular integrand φ . The next concept we recall is the recursively defined Hardy–Krause variation [24, Def. (5.8)]:

$$(6) \quad V_{\text{HK}}(\varphi) := \int_{[0, 1]^d} \left| \left(\prod_{i=1}^d \frac{\partial}{\partial z_i} \right) \varphi(\mathbf{z}) \right| d\mathbf{z} + \sum_{i=1}^d V_{\text{HK}}(\varphi(\mathbf{z})|_{z_i=1}),$$

where $\varphi(\mathbf{z})|_{z_i=1} : [0, 1]^{d-1} \rightarrow \mathbb{R}$ represents the restriction of $\varphi(\mathbf{z})$ to $\varphi(z_1, \dots, z_i = 1, \dots, z_d)$. For $\varphi : [0, 1] \rightarrow \mathbb{R}$,

$$(7) \quad V_{\text{HK}}(\varphi) := \int_{[0, 1]} \left| \frac{d}{dz} \varphi(z) \right| dz,$$

which depends on the regularity of the integrand φ and is independent of the points $\mathbf{t}^{(1)}, \dots, \mathbf{t}^{(M)}$. The mixed first-order derivatives are assumed to be continuous to guarantee the uniqueness of (6). The Koksma–Hlawka inequality [38, 26, 24] provides the following bound for the error of the QMC estimator (4)

$$(8) \quad |I - I_Q| \leq D^*(\mathbf{t}^{(1)}, \dots, \mathbf{t}^{(M)}) V_{\text{HK}}(\varphi).$$

Low-discrepancy sequences satisfying

$$(9) \quad D^*(\mathbf{t}^{(1)}, \dots, \mathbf{t}^{(M)}) = \mathcal{O}(M^{-1} \log(M)^{d-1})$$

are provided in [26]. To suppress log terms in the notation, the bound (9) can be written as follows:

$$(10) \quad D^*(\mathbf{t}^{(1)}, \dots, \mathbf{t}^{(M)}) \leq C_{\epsilon, d} M^{-1+\epsilon},$$

for any $\epsilon > 0$, where $C_{\epsilon, d} > 0$ is independent of M , and $C_{\epsilon, d} \rightarrow \infty$ as $\epsilon \rightarrow 0$. Two common low-discrepancy sequences are digital sequences [26, 47, 27, 30] and rank-1 lattice rules [25]. The concept behind digital sequences is to split $[0, 1]^d$ into equally spaced subintervals as follows:

$$(11) \quad \prod_{i=1}^d \left[\frac{a_i}{2^{b_i}}, \frac{a_i + 1}{2^{b_i}} \right),$$

where a_i, b_i are integers, with $b_i \geq 0$, $0 \leq a_i \leq 2^{b_i}$, and $1 \leq i \leq d$ such that each subinterval contains the same fraction of each nonoverlapping block of M points in the sequence. A number of points M , such that $\log_2(M) \in \mathbb{N}$, must be used to achieve the best results for this sequence type (for details on the construction of such sequences, refer to [30]). Although this study uses digital sequences to construct the (r)QMC estimators, it also presents the explicit construction of rank-1 lattice rules for illustration. Rank-1 lattice rules employ a carefully selected generating vector $\mathbf{w} \in [0, 1]^d$ to generate points $\mathbf{t}^{(m)} = \text{mod}(\frac{(m-1)\mathbf{w}}{M}; 1)$, $1 \leq m \leq M$, where $\text{mod}(\cdot; 1)$ is the componentwise modulo-1 operator in dimension d .

The deterministic QMC method introduced above has several practical disadvantages. The estimator (4) is biased, and the first point $\mathbf{t}^{(1)}$ is the origin for many common low-discrepancy sequences, which is problematic for standard classes of integrands (see Remark 1). The QMC method suffers from the curse of dimensionality for a finite number of points M but an increasing dimension d . Furthermore, the Hardy–Krause variation V_{HK} is challenging to compute. Most importantly, the QMC error in (8) is finite for some integrands for which V_{HK} is infinite [37]. A critical class of such integrands is the set of functions with singularities at one or more corners of the domain $[0, 1]^d$ (e.g., the log or inverse CDF of the normal distribution; Remark 1). A more accurate bound is provided in Owen [42], depending on how fast the mixed derivatives of the integrand increase when approaching the boundary.

2.3. Randomized Quasi-Monte Carlo method. A popular strategy for obtaining a computable error estimate for QMC methods is using points from randomized low-discrepancy sequences. Randomization also removes bias and ensures that the origin is included with only negligible probability. The deterministic points $\mathbf{t}^{(1)}, \dots, \mathbf{t}^{(M)}$ are mapped via randomization, denoted by $\boldsymbol{\rho}$, to obtain randomized low-discrepancy points $\mathbf{x}^{(m)} = \boldsymbol{\rho}(\mathbf{t}^{(m)})$, where $1 \leq m \leq M$ and the same randomization $\boldsymbol{\rho}$ is applied to each point. Thus, the points $\mathbf{x}^{(1)}, \dots, \mathbf{x}^{(M)}$ are uniformly distributed on $[0, 1]^d$ but are not independent. We applied Owen's scrambling for digital sequences [26, 47, 27] throughout this work, in which a random permutation $\boldsymbol{\rho}_{\text{sc}}$ is applied to the base two digits of $\mathbf{t}^{(m)}$, where $1 \leq m \leq M$, to build on the error bounds derived in [42, 45] for these low-discrepancy sequences. This randomization scheme is only guaranteed to preserve the low discrepancy with probability one (refer to [47, 30] for details). More specifically, we applied the Sobol sequence [32] throughout this work because it performs well on numerical tests. Another randomization scheme, in a simpler form, is presented for exposition. The random shift modulo 1 [59, 25]; that is,

$$(12) \quad \boldsymbol{\rho}_{\text{sh}}(\mathbf{t}^{(m)}) := \text{mod}(\mathbf{t}^{(m)} + \mathbf{v}; 1), \quad \mathbf{v} \sim \mathcal{U}([0, 1]^d), \quad 1 \leq m \leq M,$$

always preserves the low-discrepancy structure of the underlying points (for digital sequences or rank-1 lattice rules). Moreover, multiple randomizations $\boldsymbol{\rho}_{\text{sh}}^{(1)}, \dots, \boldsymbol{\rho}_{\text{sh}}^{(R)}$ use iid shifts $\mathbf{v}^{(r)}$, where $1 \leq r \leq R$. Using a particular randomization $\boldsymbol{\rho}$, the rQMC estimator is given by

$$(13) \quad I_{\text{rQ}} := \frac{1}{R} \sum_{r=1}^R \frac{1}{M} \sum_{m=1}^M \varphi(\mathbf{x}^{(r,m)}),$$

and the shortened notation is

$$(14) \quad \mathbf{x}^{(r,m)} := \boldsymbol{\rho}^{(r)}(\mathbf{t}^{(m)}), \quad 1 \leq r \leq R, \quad 1 \leq m \leq M.$$

The applications of rQMC methods in practice often involve integrands with an unbounded Hardy–Krause variation. Thus, a modified version of [42, Thm. 5.7] is presented, providing an error bound for integrands that do not increase too rapidly as their argument approaches the boundary of the integration domain. A recent work [43] derived a nonasymptotic error bound to account for the fact that optimal rQMC rates are typically not observed for a finite M because of the log term in (9) and also provides a minor correction to [42]. Here, we carefully track constant terms appearing in these error estimates, which will allow for the analysis of integral approximations nested in other integral approximations (33).

Assumption 1 (Boundary growth condition). *Let $\mathbf{x}^{(m)} \sim \mathcal{U}([0, 1]^d)$, where $1 \leq m \leq M$, be from a randomized low-discrepancy sequence with one randomization such that $\mathbb{E}[D^*(\mathbf{x}^{(1)}, \dots, \mathbf{x}^{(M)})] \leq C_{\epsilon,d} M^{-1+\epsilon}$ for all $\epsilon > 0$, where $C_{\epsilon,d} > 0$ is independent of M , and $C_{\epsilon,d} \rightarrow \infty$ as $\epsilon \rightarrow 0$. Furthermore, let $\varphi : [0, 1]^d \rightarrow \mathbb{R}$, such that*

$$(15) \quad \left| \left(\prod_{j \in u} \frac{\partial^u}{\partial z_j} \right) \varphi(\mathbf{z}) \right| \leq b \prod_{i=1}^d \min(z_i, 1 - z_i)^{-A_i - \mathbb{1}_{\{i \in u\}}}$$

for all $\mathbf{z} = (z_1, \dots, z_d) \in (0, 1)^d$, and all $u \subseteq \{1, \dots, d\}$, $0 < b < \infty$, $A_i > 0$, $1 \leq i \leq d$, and $\max_i A_i < 1/2$, with the convention that $(\prod_{j \in u} \partial^u / \partial z_j) \varphi \equiv \varphi$ for $u = \emptyset$.

Observe that Assumption 1 implies that $\varphi \in L^2([0, 1]^d)$.

Proposition 1 (Thm. 5.7 in [42]). *Given Assumption 1, the rQMC estimator 13 satisfies the following $L^1([0, 1]^d)$ error bound:*

$$(16) \quad \mathbb{E}[|I - I_{\text{rQ}}|] \leq b B_A C_{\epsilon,d} M^{-1+\epsilon+\max_i A_i},$$

for all $\epsilon > 0$, where $0 < b < \infty$, $B_A > 0$, $B_A \rightarrow \infty$ as $\min_i A_i \rightarrow 0$, $C_{\epsilon,d} > 0$, and $C_{\epsilon,d} \rightarrow \infty$ as $\epsilon \rightarrow 0$.

The following extension of this result for the $L^2([0, 1]^d)$ error was provided in [45],

Proposition 2 (Thm. 3.1 in [45]). *Given Assumption 1, the rQMC estimator 13 satisfies the following $L^2([0, 1]^d)$ error bound:*

$$(17) \quad \mathbb{E}[|I - I_{\text{rQ}}|^2]^{\frac{1}{2}} \leq b B_A C_{\epsilon,d} M^{-1+\epsilon+\max_i A_i},$$

for all $\epsilon > 0$, where $0 < b < \infty$, $B_A > 0$, $B_A \rightarrow \infty$ as $\min_i A_i \rightarrow 0$, $C_{\epsilon,d} > 0$, and $C_{\epsilon,d} \rightarrow \infty$ as $\epsilon \rightarrow 0$.

The difference between the estimators (2) and (13) is in the points used to evaluate the function to be integrated. For practical purposes, we employed R independent randomizations of the same low-discrepancy sequence, $\mathbf{x}^{(r,1)}, \dots, \mathbf{x}^{(r,M)}$, where $1 \leq r \leq R$, to acquire an error bound using the Chebyshev inequality; that is,

$$(18) \quad \mathbb{P} \left(|I - I_{\text{rQ}}| \leq C_\alpha \sqrt{\mathbb{V}[I_{\text{rQ}}]} \right) \geq 1 - \alpha$$

for $\alpha \in (0, 1)$, where $C_\alpha = 1/\sqrt{\alpha}$. For practical reasons, as also used in Section 4 for example, the variance of the rQMC estimator (13) can be estimated using the sample variance:

$$(19) \quad \tilde{\mathbb{V}}[I_{\text{rQ}}] := \frac{1}{R(R-1)} \sum_{r=1}^R \left(\frac{1}{M} \sum_{m=1}^M \varphi(\mathbf{x}^{(r,m)}) - I_{\text{rQ}} \right)^2.$$

For certain functions φ with desirable properties, such as smoothness and boundedness, more precise statements are possible [35, 39]. A CLT-based error estimate similar to (18) only holds asymptotically as $R \rightarrow \infty$. The estimate can still be used in practice to obtain a confidence interval of the error in (18); however, keeping R fixed and letting $M \rightarrow \infty$ is occasionally problematic, as noted in [28, 34]. Specifically, the convergence of the distribution of the estimator (13) to a normal distribution is not guaranteed.

Remark 1 (Integration over general domains). *The rQMC method is commonly defined for integration over the unit cube and uniform random variables. For integrals over general domains (e.g., normally distributed random variables), the corresponding inverse CDF can be applied to maintain the general shape of the estimators (2) and (13). This approach introduces singularities at the boundaries, leading to an unbounded Hardy–Krause variation (6). Thus, Proposition 1 or Proposition 2 is required to obtain meaningful error bounds rather than relying on the Koksma–Hlawka inequality (8).*

3. NESTED INTEGRATION

The previous section discusses the fundamentals of the rQMC estimator (13). Next, this section resumes the primary focus of this work, establishing the rDLQMC estimator (30) for nested integration problems with a discretized integrand, deriving asymptotic error bounds in the number of samples and discretization parameters, and analyzing the optimal work for this estimator to meet a tolerance goal.

Definition 1 (Nested integral). *A nested integral is defined as follows:*

$$(20) \quad \begin{aligned} I &= \int_{[0,1]^{d_1}} f \left(\int_{[0,1]^{d_2}} g(\mathbf{y}, \mathbf{x}) \, d\mathbf{x} \right) \, d\mathbf{y}, \\ &= \int_{[0,1]^{d_1}} \tilde{f}(\mathbf{y}) \, d\mathbf{y}, \end{aligned}$$

where

$$(21) \quad \tilde{f}(\mathbf{y}) := f \left(\int_{[0,1]^{d_2}} g(\mathbf{y}, \mathbf{x}) \, d\mathbf{x} \right),$$

and $f : \mathbb{R} \rightarrow \mathbb{R}$ is nonlinear. Furthermore, $g : [0, 1]^{d_1} \times [0, 1]^{d_2} \rightarrow \mathbb{R}$ defines a nonlinear relation between $\mathbf{x} \in [0, 1]^{d_2}$ and $\mathbf{y} \in [0, 1]^{d_1}$, where d_1, d_2 are positive integers.

Remark 2 (Application: expected information gain). *The following integral is nested:*

$$(22) \quad I = \int_{[0,1]^{d_1}} \log \left(\frac{1}{\det(2\pi\Sigma)^{\frac{1}{2}}} \int_{[0,1]^{d_2}} e^{-\frac{1}{2} \|\mathbf{G}(\mathbf{y}_1) + \Sigma^{\frac{1}{2}} \Phi^{-1}(\mathbf{y}_2) - \mathbf{G}(\mathbf{x})\|_{\Sigma^{-1}}^2} \, d\mathbf{x} \right) \, d\mathbf{y},$$

where

$$(23) \quad g(\mathbf{y}, \mathbf{x}) = \frac{1}{\det(2\pi\Sigma)^{\frac{1}{2}}} e^{-\frac{1}{2} \|\mathbf{G}(\mathbf{y}_1) + \Sigma^{\frac{1}{2}} \Phi^{-1}(\mathbf{y}_2) - \mathbf{G}(\mathbf{x})\|_{\Sigma^{-1}}^2},$$

and $f \equiv \log$. In these equations, \mathbf{G} denotes a nonlinear function, $d_1 > d_2$, $\mathbf{y} = (\mathbf{y}_1, \mathbf{y}_2) \in [0, 1]^{d_1}$, where $\mathbf{y}_1, \mathbf{x} \in [0, 1]^{d_2}$, $\mathbf{y}_2 \in [0, 1]^{d_1-d_2}$, and $\Sigma \in \mathbb{R}^{(d_1-d_2) \times (d_1-d_2)}$ is a positive definite matrix. Furthermore, Φ^{-1} is the inverse CDF of the standard normal in dimension $d_1 - d_2$. The integral (22) is typically not solvable in

closed form, motivating the application of numerical integration techniques to approximate I . This integral appears in the EIG, which is applied as a utility function in OED. In this context, \mathbf{G} represents a model of the experiment and regularly necessitates the solution of a PDE, motivating a FEM discretization:

$$(24) \quad \begin{aligned} g(\mathbf{y}, \mathbf{x}) &\approx g_h(\mathbf{y}, \mathbf{x}), \\ &:= \frac{1}{\det(2\pi\boldsymbol{\Sigma})^{\frac{1}{2}}} e^{-\frac{1}{2}\|\mathbf{G}_h(\mathbf{y}_1) + \boldsymbol{\Sigma}^{\frac{1}{2}}\Phi^{-1}(\mathbf{y}_2) - \mathbf{G}_h(\mathbf{x})\|_{\boldsymbol{\Sigma}^{-1}}^2}, \end{aligned}$$

where \mathbf{G}_h , $h > 0$, denotes the FEM approximation of \mathbf{G} (see Assumption 2). Furthermore, \mathbf{x} and \mathbf{y}_1 are parameters of interest, and $\boldsymbol{\Sigma}^{\frac{1}{2}}\Phi^{-1}(\mathbf{y}_2)$ denotes the observation noise.

Remark 3 (Nested integral). If f in (20) is linear, the nested integral (20) simplifies to a nonnested integral in dimension $d_1 + d_2$. If g is separable (i.e., $g(\mathbf{y}, \mathbf{x}) \equiv g_1(\mathbf{y})g_2(\mathbf{x})$, for some functions g_1 and g_2), then the inner and outer integral in (20) can be separately approximated. Numerical approximation schemes are substantially more efficient in these cases than for truly nested integrals.

The following DLMC estimator [1] results from a standard Double Loop MC method to approximate a nested integral (20):

$$(25) \quad I_{\text{DLMC}} := \frac{1}{N} \sum_{n=1}^N f \left(\frac{1}{M} \sum_{m=1}^M g(\mathbf{y}^{(n)}, \mathbf{x}^{(n,m)}) \right),$$

where the points $\mathbf{y}^{(n)}$, where $1 \leq n \leq N$, are iid and sampled from $\mathcal{U}([0, 1]^{d_1})$, and $\mathbf{x}^{(n,m)}$, where $1 \leq n \leq N$, and $1 \leq m \leq M$, are iid and sampled from $\mathcal{U}([0, 1]^{d_2})$. The standard MC estimator (2) for a single integral is unbiased and has a variance that decreases with the number of samples, which holds for the inner MC estimator in (25), where the variance decreases with the number of inner samples M . The outer MC estimator in (25) has a variance that decreases with N and has a bias relative to the size of the variance of the inner integral estimate. Thus, many inner and outer samples are typically required to control the bias and variance of this estimator, significantly limiting its practical usefulness, predominantly for computationally demanding problems.

Directly evaluating the function g is often not feasible. For example, if evaluating g requires solving a PDE, only a FEM approximation g_h with a discretization parameter h may be accessible. Thus, the following assumption is made.

Assumption 2 (Discretization rate). Let g_h be an approximation of g such that

$$(26) \quad |\mathbb{E}[g(\mathbf{y}, \mathbf{x}) - g_h(\mathbf{y}, \mathbf{x})]| \leq C_{\text{disc}} h^\eta,$$

where $\eta > 0$ denotes the h -convergence rate, and $C_{\text{disc}} > 0$ is constant in h . The work of evaluating g_h is assumed to be of order $\mathcal{O}(h^{-\gamma})$, for some $\gamma > 0$.

Moreover, the variance of the DLMC estimator (25) for discretized integrand g_h is assumed to be finite as $h \rightarrow 0$. Unless stated otherwise, a discretized version g_h is applied in the numerical estimators, and the subscript was omitted for simplicity thereafter. For square-integrable and thrice-differentiable f and square-integrable g , the bias of the DLMC estimator has the following upper bound:

$$(27) \quad |\mathbb{E}[I_{\text{DLMC}}] - I| \leq C_{\text{disc}} h^\eta + \frac{C_{\text{MC},3}}{M},$$

where $C_{\text{MC},3} > 0$ represents a constant related to the variance of the inner MC estimation in (25), and $C_{\text{disc}} > 0$ could be different from that introduced in Assumption 2. Furthermore, the variance of the DLMC estimator has the following upper bound:

$$(28) \quad \mathbb{V}[I_{\text{DLMC}}] \leq \frac{C_{\text{MC},1}}{N} + \frac{C_{\text{MC},2}}{NM},$$

where $C_{\text{MC},1}, C_{\text{MC},2} > 0$ are constants [2]. The optimal work of the DLMC estimator for a specific error tolerance $TOL > 0$ is given by

$$(29) \quad W_{\text{DLMC}}^* = \mathcal{O} \left(TOL^{-\left(3 + \frac{\gamma}{\eta}\right)} \right),$$

as $TOL \rightarrow 0$. Proofs for the specific case of approximating the EIG in Bayesian OED are provided in [2], and adapting them to the general case of a nested integral is straightforward. Proofs for general integrands

without additional inner discretization (e.g., FEM) are provided in [49], where nonsmooth integrands are also considered. These proofs assume that the outer integrand is thrice differentiable; however, this is not a requirement for the estimator (25) to converge. In [48], similar error bounds were derived using more lenient requirements.

To attain smaller error bounds and optimal work, in this work we replace both MC approximations in (25) with rQMC approximations and arrived at the rDLQMC estimator, defined below.

Definition 2 (rDLQMC estimator). *The rDLQMC estimator of a nested integral (20) is defined as follows:*

$$(30) \quad I_{\text{rDLQ}}^{(S,R)} := \frac{1}{S} \sum_{s=1}^S \frac{1}{N} \sum_{n=1}^N f \left(\frac{1}{R} \sum_{r=1}^R \frac{1}{M} \sum_{m=1}^M g(\mathbf{y}^{(s,n)}, \mathbf{x}^{(n,r,m)}) \right),$$

where $f : \mathbb{R} \rightarrow \mathbb{R}$ is nonlinear, and $g : [0, 1]^{d_1} \times [0, 1]^{d_2} \rightarrow \mathbb{R}$ defines a nonlinear relation between \mathbf{x} and \mathbf{y} . The samples take the following shape

$$(31) \quad \mathbf{y}^{(s,n)} := \boldsymbol{\rho}^{(s)}(\mathbf{u}^{(n)}), \quad 1 \leq s \leq S, 1 \leq n \leq N,$$

where $\boldsymbol{\rho}^{(s)}$, with $1 \leq s \leq S$, is the independent randomization of points in a digital sequence $\mathbf{u}^{(1)}, \dots, \mathbf{u}^{(N)}$ in d_1 , using Owen's scrambling, and

$$(32) \quad \mathbf{x}^{(s,n,r,m)} := \boldsymbol{\rho}^{(s,n,r)}(\mathbf{t}^{(m)}), \quad 1 \leq s \leq S, 1 \leq n \leq N, 1 \leq r \leq R, 1 \leq m \leq M,$$

where $\boldsymbol{\rho}^{(s,n,r)}$, with $1 \leq s \leq S, 1 \leq n \leq N$, and $1 \leq r \leq R$ are independent randomizations of points in a digital sequence $\mathbf{t}^{(1)}, \dots, \mathbf{t}^{(M)}$ in d_2 , using Owen's scrambling.

Remark 4 (Number of randomizations). *Increasing the number of randomizations R and S in the estimator (30) reduces the bias and statistical error at the (MC) rates in (27) and (28), respectively. Only one randomization (i.e., scramble) of the outer samples in the estimator in (33) was applied, and numerous low-discrepancy points N and M were employed to maximize the effect of the low-discrepancy structure. Choosing independent randomizations of the inner samples for each outer sample enables the bounding of the variance in Proposition (4). The rDLQMC estimator with one randomization is introduced below to avoid clutter and is applied throughout the following propositions. For practical applications, including the numerical experiments in Section 4, the variance contribution of the inner and outer estimators was estimated separately, using pilot runs with a fixed number of randomizations $S, R > 1$.*

Definition 3 (rDLQMC estimator with $S, R = 1$). *The rDLQMC estimator for a nested integral (20) with $S, R = 1$ is defined as follows:*

$$(33) \quad \begin{aligned} I_{\text{rDLQ}} &:= I_{\text{rDLQ}}^{(1,1)}, \\ &= \frac{1}{N} \sum_{n=1}^N f \left(\frac{1}{M} \sum_{m=1}^M g(\mathbf{y}^{(n)}, \mathbf{x}^{(n,m)}) \right), \end{aligned}$$

where $f : \mathbb{R} \rightarrow \mathbb{R}$ is nonlinear, and $g : [0, 1]^{d_1} \times [0, 1]^{d_2} \rightarrow \mathbb{R}$ defines a nonlinear relation between \mathbf{x} and \mathbf{y} . The samples take the following shape:

$$(34) \quad \mathbf{y}^{(n)} := \boldsymbol{\rho}(\mathbf{u}^{(n)}), \quad 1 \leq n \leq N,$$

where $\boldsymbol{\rho}$ is a randomization of points in a digital sequence $\mathbf{u}^{(1)}, \dots, \mathbf{u}^{(N)}$ in d_1 , applying Owen's scrambling, and

$$(35) \quad \mathbf{x}^{(n,m)} := \boldsymbol{\rho}^{(n)}(\mathbf{t}^{(m)}), \quad 1 \leq n \leq N, 1 \leq m \leq M,$$

where $\boldsymbol{\rho}^{(n)}$, with $1 \leq n \leq N$, are independent randomizations of points in a digital sequence $\mathbf{t}^{(1)}, \dots, \mathbf{t}^{(M)}$ in d_2 , applying Owen's scrambling.

Next, we analyze the error of the rDLQMC method. For this purpose, the error is split into bias and statistical errors, respectively, and each is estimated individually, as follows:

$$(36) \quad |I_{\text{rDLQ}} - I| \leq \underbrace{|\mathbb{E}[I_{\text{rDLQ}}] - I|}_{\text{bias error}} + \underbrace{|I_{\text{rDLQ}} - \mathbb{E}[I_{\text{rDLQ}}]|}_{\text{statistical error}}.$$

The following notation is defined:

$$(37) \quad \hat{g}_M(\mathbf{y}) := \frac{1}{M} \sum_{m=1}^M g(\mathbf{y}, \mathbf{x}^{(m)}),$$

$$(38) \quad \begin{aligned} \bar{g}(\mathbf{y}) &:= \mathbb{E}[\hat{g}_M(\mathbf{y})|\mathbf{y}], \\ &= \mathbb{E}[g(\mathbf{y}, \mathbf{x})|\mathbf{y}], \\ &= \int_{[0,1]^{d_2}} g(\mathbf{y}, \mathbf{x}) \, d\mathbf{x}, \end{aligned}$$

where the conditioning is on the randomization $\boldsymbol{\rho}$ of the outer variable $\mathbf{y} = \boldsymbol{\rho}(\mathbf{u})$, and

$$(39) \quad \Delta g_M(\mathbf{y}) := \hat{g}_M(\mathbf{y}) - \bar{g}(\mathbf{y}),$$

where the dependence on $\mathbf{x}^{(m)}$, where $1 \leq m \leq M$, is suppressed, and the index n is omitted for brevity. Next, the assumptions for establishing the bound on the bias error of the rDLQMC estimator are presented.

Assumption 3 (Integrability assumption for the composition of the outer and inner integrand). *Let $\tilde{f}(\cdot) \equiv f(K\bar{g}(\cdot)) : [0, 1]^{d_1} \rightarrow \mathbb{R}$, where $0 < K < 2$, with \bar{g} as in (38) be an element of the Sobolev space $W^{3,p}([0, 1]^{d_1})$, for some p , where $1 \leq p \leq \infty$.*

Assumption 4 (Inverse inequality for the inner integrand). *Let $g(\cdot, \cdot) : [0, 1]^{d_1} \times [0, 1]^{d_2} \rightarrow \mathbb{R}$ such that*

$$(40) \quad \sup_{\mathbf{y} \in [0,1]^{d_1}} \left| \frac{V_{\text{HK}}(g(\mathbf{y}, \cdot))}{\bar{g}(\mathbf{y})} \right| < k < \infty,$$

for some constant k , with V_{HK} as in (6) and \bar{g} as in (38). Furthermore, if Assumption 3 holds, let $\bar{g} \in L^{3q}([0, 1]^{d_1})$ for some q , such that $1 \leq q \leq \infty$, with $1/p + 1/q = 1$, and p as in Assumption 3.

Proposition 3 (Bias of the rDLQMC estimator). *Given Assumptions 2–4, if $|f'''|$ is monotonic, the bias of the rDLQMC estimator (33) has the following upper bound:*

$$(41) \quad |\mathbb{E}[I_{\text{rDLQ}}] - I| \leq C_{\text{disc}} h^\eta + \frac{\mathbb{E}[|\bar{g}|^2 |f''(\bar{g})|] k^2 C_{\epsilon, d_2}^2}{2M^{2-2\epsilon}} + \frac{\mathbb{E}[|\bar{g}|^3 |f'''(K\bar{g})|] k^3 C_{\epsilon, d_2}^3}{6M^{3-3\epsilon}},$$

for any $\epsilon > 0$, $0 < k < \infty$, and $0 < K < 2$, where $C_{\epsilon, d_2} \rightarrow \infty$ as $\epsilon \rightarrow 0$.

Proof. First, $I_{\text{rDLQ}}^{\text{ex}} = \lim_{h \rightarrow 0^+} I_{\text{rDLQ}}$ ¹ is introduced, which is the rDLQMC estimator for g evaluated exactly. Further, the bias is split into the following:

$$(42) \quad |\mathbb{E}[I_{\text{rDLQ}}] - I| \leq \underbrace{|\mathbb{E}[I_{\text{rDLQ}} - I_{\text{rDLQ}}^{\text{ex}}]|}_{\text{discretization bias}} + \underbrace{|\mathbb{E}[I_{\text{rDLQ}}^{\text{ex}}] - I|}_{\text{inner sampling bias}}.$$

For the discretization bias,

$$(43) \quad |\mathbb{E}[I_{\text{rDLQ}} - I_{\text{rDLQ}}^{\text{ex}}]| \leq C_{\text{disc}} h^\eta$$

by Assumption 2. For the bias from the inner sampling, the following Taylor expansion for $f(\hat{g}_M(\mathbf{y}))$ around $\bar{g}(\mathbf{y})$ is considered:

$$(44) \quad \begin{aligned} f(\hat{g}_M(\mathbf{y})) - f(\bar{g}(\mathbf{y})) &= f'(\bar{g}(\mathbf{y})) \Delta g_M(\mathbf{y}) + \frac{1}{2} f''(\bar{g}(\mathbf{y})) (\Delta g_M(\mathbf{y}))^2 \\ &\quad + \frac{1}{2} (\Delta g_M(\mathbf{y}))^3 \int_0^1 f'''(\bar{g}(\mathbf{y}) + s \Delta g_M(\mathbf{y})) (1-s)^2 \, ds. \end{aligned}$$

The absolute value of the expectation of the left-hand side of (44) is the inner sampling bias of the rDLQMC estimator. Thus, each term on the right-hand side must be estimated. For the first term in (44),

$$(45) \quad \begin{aligned} |\mathbb{E}[f'(\bar{g}(\mathbf{y})) \Delta g_M(\mathbf{y})]| &= |\mathbb{E}[\mathbb{E}[f'(\bar{g}(\mathbf{y})) \Delta g_M(\mathbf{y})|\mathbf{y}]]|, \\ &= |\mathbb{E}[f'(\bar{g}(\mathbf{y})) \underbrace{\mathbb{E}[\Delta g_M(\mathbf{y})|\mathbf{y}]}_{=0}]|, \\ &= 0. \end{aligned}$$

¹The limit is in expectation.

For the second term in (44),

$$\begin{aligned}
\left| \mathbb{E} \left[f''(\bar{g}(\mathbf{y})) (\Delta g_M(\mathbf{y}))^2 \right] \right| &= \left| \mathbb{E} \left[\mathbb{E} \left[f''(\bar{g}(\mathbf{y})) (\Delta g_M(\mathbf{y}))^2 \middle| \mathbf{y} \right] \right] \right|, \\
(46) \qquad \qquad \qquad &= \left| \mathbb{E} \left[f''(\bar{g}(\mathbf{y})) \mathbb{E} \left[(\Delta g_M(\mathbf{y}))^2 \middle| \mathbf{y} \right] \right] \right|.
\end{aligned}$$

For the inner expectation, by Assumption 4 and the Koksma–Hlawka inequality (8),

$$\begin{aligned}
\mathbb{E} \left[(\Delta g_M(\mathbf{y}))^2 \middle| \mathbf{y} \right] &= \mathbb{E} \left[\left| \int_{[0,1]^{d_2}} g(\mathbf{y}, \mathbf{x}) \, d\mathbf{x} - \frac{1}{M} \sum_{m=1}^M g(\mathbf{y}, \mathbf{x}^{(m)}) \right|^2 \middle| \mathbf{y} \right], \\
(47) \qquad \qquad \qquad &\leq (V_{\text{HK}}(g(\mathbf{y}, \cdot)))^2 C_{\epsilon, d_2}^2 M^{-2+2\epsilon}, \\
&\leq (\bar{g}(\mathbf{y}))^2 k^2 C_{\epsilon, d_2}^2 M^{-2+2\epsilon},
\end{aligned}$$

for any $\epsilon > 0$, where $C_{\epsilon, d_2} \rightarrow \infty$ as $\epsilon \rightarrow 0$. By Hölder's inequality, combining the two previous expressions results in

$$\begin{aligned}
\left| \mathbb{E} \left[f''(\bar{g}(\mathbf{y})) (\Delta g_M(\mathbf{y}))^2 \right] \right| &\leq \mathbb{E} \left[|f''(\bar{g}(\mathbf{y}))| (\bar{g}(\mathbf{y}))^2 \right] k^2 C_{\epsilon, d_2}^2 M^{-2+2\epsilon}, \\
(48) \qquad \qquad \qquad &\leq \mathbb{E} \left[|f''(\bar{g}(\mathbf{y}))|^p \right]^{\frac{1}{p}} \mathbb{E} \left[|\bar{g}(\mathbf{y})|^{2q} \right]^{\frac{1}{q}} k^2 C_{\epsilon, d_2}^2 M^{-2+2\epsilon}, \\
&< \infty,
\end{aligned}$$

per Assumption 3 and 4. For the third term in (44),

$$\begin{aligned}
&\left| \mathbb{E} \left[(\Delta g_M(\mathbf{y}))^3 \int_0^1 f'''(\bar{g}(\mathbf{y}) + s\Delta g_M(\mathbf{y})) (1-s)^2 \, ds \right] \right|, \\
&= \left| \mathbb{E} \left[\mathbb{E} \left[(\Delta g_M(\mathbf{y}))^3 \int_0^1 f'''(\bar{g}(\mathbf{y}) + s\Delta g_M(\mathbf{y})) (1-s)^2 \, ds \middle| \mathbf{y} \right] \right] \right|, \\
(49) \qquad \qquad \qquad &\leq \mathbb{E} \left[\mathbb{E} \left[|\Delta g_M(\mathbf{y})|^3 \int_0^1 |f'''(\bar{g}(\mathbf{y}) + s\Delta g_M(\mathbf{y}))| (1-s)^2 \, ds \middle| \mathbf{y} \right] \right].
\end{aligned}$$

Owen's scrambling yields a low-discrepancy sequence with probability one. From Assumption 4, assuming that $|f'''|$ is monotonically decreasing, with probability one,

$$\begin{aligned}
\int_0^1 |f'''(\bar{g}(\mathbf{y}) + s\Delta g_M(\mathbf{y}))| (1-s)^2 \, ds &\leq \int_0^1 |f'''(\bar{g}(\mathbf{y}) - s|\Delta g_M(\mathbf{y})|)| (1-s)^2 \, ds, \\
&\leq |f'''(\bar{g}(\mathbf{y}) - |\Delta g_M(\mathbf{y})|)| \int_0^1 (1-s)^2 \, ds, \\
&= \frac{1}{3} |f'''(\bar{g}(\mathbf{y}) - |\Delta g_M(\mathbf{y})|)|, \\
&\leq \frac{1}{3} |f'''(\bar{g}(\mathbf{y}) - C_{\epsilon, d_2} M^{-1+\epsilon} V_{\text{HK}}(g(\mathbf{y}, \cdot)))|, \\
&\leq \frac{1}{3} |f'''(\bar{g}(\mathbf{y}) - C_{\epsilon, d_2} M^{-1+\epsilon} k |\bar{g}(\mathbf{y})|)|, \\
&\leq \frac{1}{3} |f'''((1 - \tilde{k})\bar{g}(\mathbf{y}))|, \\
(50) \qquad \qquad \qquad &= \frac{1}{3} |f'''(K\bar{g}(\mathbf{y}))|,
\end{aligned}$$

where $K = 1 - \tilde{k}$, with $0 \leq \tilde{k} < 1$ and $0 < K \leq 1$ for M greater than some $M_0(\tilde{k})$. Substituting it into (49) results in

$$(51) \quad \left| \mathbb{E} \left[(\Delta g_M(\mathbf{y}))^3 \int_0^1 f'''(\bar{g}(\mathbf{y}) + s\Delta g_M(\mathbf{y})) (1-s)^2 \, ds \right] \right| \leq \frac{1}{3} \mathbb{E} \left[\mathbb{E} \left[|\Delta g_M(\mathbf{y})|^3 \middle| \mathbf{y} \right] |f'''(K\bar{g}(\mathbf{y}))| \right].$$

For the inner expectation, by Assumption 4 and the Koksma–Hlawka inequality (8),

$$\begin{aligned}
\mathbb{E}[|\Delta g_M(\mathbf{y})|^3 | \mathbf{y}] &= \mathbb{E} \left[\left| \int_{[0,1]^{d_2}} g(\mathbf{y}, \mathbf{x}) \, d\mathbf{x} - \frac{1}{M} \sum_{m=1}^M g(\mathbf{y}, \mathbf{x}^{(m)}) \right|^3 \middle| \mathbf{y} \right], \\
&\leq (V_{\text{HK}}(g(\mathbf{y}, \cdot)))^3 C_{\epsilon, d_2}^3 M^{-3+3\epsilon}, \\
(52) \quad &\leq |\bar{g}(\mathbf{y})|^3 k^3 C_{\epsilon, d_2}^3 M^{-3+3\epsilon},
\end{aligned}$$

for any $\epsilon > 0$. By Hölder's inequality

$$\begin{aligned}
&\left| \mathbb{E} \left[(\Delta g_M(\mathbf{y}))^3 \int_0^1 f'''(\bar{g}(\mathbf{y}) + s\Delta g_M(\mathbf{y})) (1-s)^2 \, ds \right] \right|, \\
&\leq \frac{1}{3} \mathbb{E} [|f'''(K\bar{g}(\mathbf{y}))| |\bar{g}(\mathbf{y})|^3] k^3 C_{\epsilon, d_2}^3 M^{-3+3\epsilon}, \\
&\leq \frac{1}{3} \mathbb{E} [|f'''(K\bar{g}(\mathbf{y}))|^p]^{\frac{1}{p}} \mathbb{E} [|\bar{g}(\mathbf{y})|^{3q}]^{\frac{1}{q}} k^3 C_{\epsilon, d_2}^3 M^{-3+3\epsilon}, \\
(53) \quad &< \infty,
\end{aligned}$$

by Assumption 3 and 4. For an $|f'''|$ that is monotonically increasing, similar arguments hold where $K = 1 - \tilde{k}$, where $0 < K \leq 1$ is replaced with $K = 1 + \tilde{k}$, where $1 \leq K < 2$. \square

Remark 5 (Dependence on the dimension d_2). *Under appropriate regularity conditions, the dependence on the dimension d_2 in the above result can be neglected; cf., [63].*

The statistical error is bounded in probability by the Chebyshev inequality using the estimator variance $\mathbb{V}[I_{\text{rDLQ}}]$; that is, for

$$(54) \quad \epsilon_{\text{rDLQ}} := C_\alpha \sqrt{\mathbb{V}[I_{\text{rDLQ}}]},$$

we have

$$(55) \quad \mathbb{P}(|I_{\text{rDLQ}} - \mathbb{E}[I_{\text{rDLQ}}]| \leq \epsilon_{\text{rDLQ}}) \geq 1 - \alpha$$

for $\alpha \in (0, 1)$, where $C_\alpha = 1/\sqrt{\alpha}$. Next, the assumptions for establishing the bound on the variance of the rDLQMC estimator are presented.

Assumption 5 (Integrability assumption for the composition of the outer and inner integrand). *Let $\tilde{f}(\cdot) \equiv f(K\bar{g}_h(\cdot)) : [0, 1]^{d_1} \rightarrow \mathbb{R}$ be an element of the Sobolev space $W^{2,2p}([0, 1]^{d_1})$, with $0 < K < 2$, \bar{g}_h as in Assumption 2, and (38), for some p , where $1 \leq p \leq \infty$ as $h \rightarrow 0$.*

Assumption 6 (Inverse inequality for the inner integrand). *Let $g_h(\mathbf{y}, \mathbf{x}) : [0, 1]^{d_1} \times [0, 1]^{d_2} \rightarrow \mathbb{R}$, such that*

$$(56) \quad \sup_{\mathbf{y} \in [0, 1]^{d_1}} \left| \frac{V_{\text{HK}}(g_h(\mathbf{y}, \cdot))}{\bar{g}_h(\mathbf{y})} \right| < k < \infty,$$

for some constant k , with V_{HK} as in (6), g_h and \bar{g}_h as in Assumption 2, and (38) as $h \rightarrow 0$. Furthermore, if Assumption 5 holds, let $\bar{g}_h \in L^{4q}([0, 1]^{d_1})$ for some q , where $1 \leq q \leq \infty$, with $1/p + 1/q = 1$, and p as in Assumption 5.

Proposition 4 (Variance of the rDLQMC estimator). *For $\tilde{f} \equiv f(\bar{g}_h)$ satisfying Assumptions 1 and 5, g_h satisfying Assumption 6, if $|f''|$ is monotonic, the variance of the rDLQMC estimator (33) has the following upper bound:*

$$(57) \quad \mathbb{V}[I_{\text{rDLQ}}] \leq \frac{2b^2 B_A^2 C_{\epsilon, d_1}^2}{N^{2-2\epsilon-2\max_i A_i}} + \frac{2\mathbb{E}[|\bar{g}_h|^2 |f'(\bar{g}_h)|^2] k^2 C_{\epsilon, d_2}^2}{NM^{2-2\epsilon}} + \frac{\mathbb{E}[|\bar{g}_h|^4 |f''(K\bar{g}_h)|^2] (\Gamma_{d_1} + 1) k^4 C_{\epsilon, d_2}^4}{2NM^{4-4\epsilon}},$$

for any $\epsilon > 0$, $0 < k < \infty$, and $0 < K < 2$, where $C_{\epsilon, d_1}, C_{\epsilon, d_2} \rightarrow \infty$ as $\epsilon \rightarrow 0$, $B_A \rightarrow \infty$ as $\min_i A_i \rightarrow 0$, and $\Gamma_{d_1} \rightarrow \infty$ as $d_1 \rightarrow \infty$.

Proof. The index h is omitted for simplicity, and the following Taylor expansion of $f(\hat{g}_M(\mathbf{y}))$ around $\bar{g}(\mathbf{y})$ is considered:

$$(58) \quad f(\hat{g}_M(\mathbf{y})) = f(\bar{g}(\mathbf{y})) + f'(\bar{g}(\mathbf{y}))\Delta g_M(\mathbf{y}) + (\Delta g_M(\mathbf{y}))^2 \int_0^1 f''(\bar{g}(\mathbf{y}) + s\Delta g_M(\mathbf{y})) (1-s) ds.$$

By the law of total variance, we obtain

$$(59) \quad \begin{aligned} \mathbb{V}[I_{\text{rDLQ}}] &= \mathbb{V} \left[\frac{1}{N} \sum_{n=1}^N f(\hat{g}_M(\mathbf{y}^{(n)})) \right], \\ &= \mathbb{V} \left[\mathbb{E} \left[\frac{1}{N} \sum_{n=1}^N f(\hat{g}_M(\mathbf{y}^{(n)})) \middle| \{\mathbf{y}^{(n)}\}_{n=1}^N \right] \right] + \mathbb{E} \left[\mathbb{V} \left[\frac{1}{N} \sum_{n=1}^N f(\hat{g}_M(\mathbf{y}^{(n)})) \middle| \{\mathbf{y}^{(n)}\}_{n=1}^N \right] \right], \end{aligned}$$

where conditioning occurs on the randomization $\boldsymbol{\rho}$ of the outer random variables $\mathbf{y}^{(n)} = \boldsymbol{\rho}(\mathbf{u}^{(n)})$, where $1 \leq n \leq N$. Moreover, using (58) for the first term in (59) yields the following:

$$(60) \quad \begin{aligned} &\mathbb{V} \left[\mathbb{E} \left[\frac{1}{N} \sum_{n=1}^N f(\hat{g}_M(\mathbf{y}^{(n)})) \middle| \{\mathbf{y}^{(n)}\}_{n=1}^N \right] \right], \\ &= \mathbb{V} \left[\frac{1}{N} \sum_{n=1}^N \left(f(\bar{g}(\mathbf{y}^{(n)})) + \mathbb{E} \left[(\Delta g_M(\mathbf{y}^{(n)}))^2 \int_0^1 f''(\bar{g}(\mathbf{y}^{(n)} + s\Delta g_M(\mathbf{y}^{(n)})) (1-s) ds \middle| \mathbf{y}^{(n)} \right] \right) \right] \right], \\ &\leq 2\mathbb{V} \left[\frac{1}{N} \sum_{n=1}^N f(\bar{g}(\mathbf{y}^{(n)})) \right] + 2\mathbb{V} \left[\frac{1}{N} \sum_{n=1}^N \mathbb{E} \left[(\Delta g_M(\mathbf{y}^{(n)}))^2 \int_0^1 f''(\bar{g}(\mathbf{y}^{(n)} + s\Delta g_M(\mathbf{y}^{(n)})) (1-s) ds \middle| \mathbf{y}^{(n)} \right] \right], \end{aligned}$$

where the last line follows from the Cauchy–Schwarz inequality (see Appendix A). For the first term in (60), we have

$$(61) \quad \begin{aligned} 2\mathbb{V} \left[\frac{1}{N} \sum_{n=1}^N f(\bar{g}(\mathbf{y}^{(n)})) \right] &= 2\mathbb{E} \left[\left| \frac{1}{N} \sum_{n=1}^N f(\bar{g}(\mathbf{y}^{(n)})) - \int_{[0,1]^{d_1}} f(\bar{g}(\mathbf{y})) d\mathbf{y} \right|^2 \right], \\ &\leq 2b^2 B_A^2 C_{\epsilon, d_1}^2 N^{-2+2\epsilon+2\max_i A_i}, \end{aligned}$$

by Assumption 1 and Proposition 2. For the second term in (60), the variance of scrambled points from a digital sequence is bounded by the MC variance times a constant $\Gamma_{d_1} > 0$, where $\Gamma_{d_1} \rightarrow \infty$ as $d_1 \rightarrow \infty$ [58, 60]; thus

$$(62) \quad \begin{aligned} &2\mathbb{V} \left[\frac{1}{N} \sum_{n=1}^N \mathbb{E} \left[(\Delta g_M(\mathbf{y}^{(n)}))^2 \int_0^1 f''(\bar{g}(\mathbf{y}^{(n)} + s\Delta g_M(\mathbf{y}^{(n)})) (1-s) ds \middle| \mathbf{y}^{(n)} \right] \right], \\ &\leq 2\Gamma_{d_1} \mathbb{V} \left[\frac{1}{N} \sum_{n=1}^N \mathbb{E} \left[(\Delta g_M(\mathbf{z}^{(n)}))^2 \int_0^1 f''(\bar{g}(\mathbf{z}^{(n)} + s\Delta g_M(\mathbf{z}^{(n)})) (1-s) ds \middle| \mathbf{z}^{(n)} \right] \right], \end{aligned}$$

where $\mathbf{z}^{(n)}$, with $1 \leq n \leq N$, is iid in $[0, 1]^{d_1}$. From this, we obtain

$$(63) \quad \begin{aligned} &2\Gamma_{d_1} \mathbb{V} \left[\frac{1}{N} \sum_{n=1}^N \mathbb{E} \left[(\Delta g_M(\mathbf{z}^{(n)}))^2 \int_0^1 f''(\bar{g}(\mathbf{z}^{(n)} + s\Delta g_M(\mathbf{z}^{(n)})) (1-s) ds \middle| \mathbf{z}^{(n)} \right] \right], \\ &= \frac{2\Gamma_{d_1}}{N} \mathbb{V} \left[\mathbb{E} \left[(\Delta g_M(\mathbf{z}))^2 \int_0^1 f''(\bar{g}(\mathbf{z} + s\Delta g_M(\mathbf{z})) (1-s) ds \middle| \mathbf{z} \right] \right], \\ &\leq \frac{2\Gamma_{d_1}}{N} \mathbb{E} \left[\left| \mathbb{E} \left[(\Delta g_M(\mathbf{z}))^2 \int_0^1 f''(\bar{g}(\mathbf{z} + s\Delta g_M(\mathbf{z})) (1-s) ds \middle| \mathbf{z} \right] \right|^2 \right], \\ &\leq \frac{2\Gamma_{d_1}}{N} \mathbb{E} \left[\mathbb{E} \left[|\Delta g_M(\mathbf{z})|^4 \left(\int_0^1 |f''(\bar{g}(\mathbf{z} + s\Delta g_M(\mathbf{z}))| (1-s) ds \right)^2 \middle| \mathbf{z} \right] \right]. \end{aligned}$$

With an argument similar to that in (50), by Assumption 6 and because $|f''|$ is monotonic,

$$(64) \quad \int_0^1 |f''(\bar{g}(\mathbf{z}) + s\Delta g_M(\mathbf{z}))| (1-s) ds \leq \frac{1}{2} |f''(K\bar{g}(\mathbf{z}))|,$$

where $0 < K < 2$ for a sufficiently large M . Substituting this into (63) results in the following:

$$(65) \quad \begin{aligned} & \frac{2\Gamma_{d_1}}{N} \mathbb{E} \left[\mathbb{E} \left[|\Delta g_M(\mathbf{z})|^4 \left(\int_0^1 |f''(\bar{g}(\mathbf{z}) + s\Delta g_M(\mathbf{z}))| (1-s) ds \right)^2 \middle| \mathbf{z} \right] \right], \\ & \leq \frac{\Gamma_{d_1}}{2N} \mathbb{E} \left[\mathbb{E} \left[|\Delta g_M(\mathbf{z})|^4 \middle| \mathbf{z} \right] |f''(K\bar{g}(\mathbf{z}))|^2 \right]. \end{aligned}$$

For the inner expectation, by Assumption 6 and the Koksma–Hlawka inequality (8),

$$(66) \quad \begin{aligned} \mathbb{E}[|\Delta g_M(\mathbf{z})|^4 | \mathbf{z}] &= \mathbb{E} \left[\left| \int_{[0,1]^{d_2}} g(\mathbf{z}, \mathbf{x}) d\mathbf{x} - \frac{1}{M} \sum_{m=1}^M g(\mathbf{z}, \mathbf{x}^{(m)}) \right|^4 \middle| \mathbf{z} \right], \\ &\leq (V_{\text{HK}}(g(\mathbf{z}, \cdot)))^4 C_{\epsilon, d_2}^4 M^{-4+4\epsilon}, \\ &\leq |\bar{g}(\mathbf{z})|^4 k^4 C_{\epsilon, d_2}^4 M^{-4+4\epsilon}, \end{aligned}$$

for any $\epsilon > 0$. Combining the previous two expressions, by Hölder's inequality,

$$(67) \quad \begin{aligned} \frac{\Gamma_{d_1}}{2N} \mathbb{E} \left[\mathbb{E} \left[|\Delta g_M(\mathbf{z})|^4 \middle| \mathbf{z} \right] |f''(K\bar{g}(\mathbf{z}))|^2 \right] &\leq \frac{\Gamma_{d_1}}{2N} \mathbb{E} \left[|\bar{g}(\mathbf{z})|^4 |f''(K\bar{g}(\mathbf{z}))|^2 \right] k^4 C_{\epsilon, d_2}^4 M^{-4+4\epsilon}, \\ &\leq \frac{\Gamma_{d_1}}{2N} \mathbb{E} \left[|\bar{g}(\mathbf{z})|^{4q} \right]^{\frac{1}{q}} \mathbb{E} \left[|f''(K\bar{g}(\mathbf{z}))|^{2p} \right]^{\frac{1}{p}} k^4 C_{\epsilon, d_2}^4 M^{-4+4\epsilon}, \\ &< \infty, \end{aligned}$$

by Assumption 5 and 6. For the second term in (59), using (58) yields the following:

$$(68) \quad \begin{aligned} & \mathbb{E} \left[\mathbb{V} \left[\frac{1}{N} \sum_{n=1}^N f(\hat{g}_M(\mathbf{y}^{(n)})) \middle| \{\mathbf{y}^{(n)}\}_{n=1}^N \right] \right] = \frac{1}{N^2} \sum_{n=1}^N \mathbb{E} \left[\mathbb{V} \left[f(\hat{g}_M(\mathbf{y}^{(n)})) \middle| \mathbf{y}^{(n)} \right] \right], \\ &= \frac{1}{N} \mathbb{E} \left[\mathbb{V} \left[f(\hat{g}_M(\mathbf{y})) \middle| \mathbf{y} \right] \right], \\ &= \frac{1}{N} \mathbb{E} \left[\mathbb{V} \left[f'(\bar{g}(\mathbf{y}))\Delta g_M(\mathbf{y}) + (\Delta g_M(\mathbf{y}))^2 \int_0^1 f''(\bar{g}(\mathbf{y}) + s\Delta g_M(\mathbf{y})) (1-s) ds \middle| \mathbf{y} \right] \right], \\ &\leq \frac{2}{N} \mathbb{E} \left[\mathbb{V} \left[f'(\bar{g}(\mathbf{y}))\Delta g_M(\mathbf{y}) \middle| \mathbf{y} \right] \right] + \frac{2}{N} \mathbb{E} \left[\mathbb{V} \left[(\Delta g_M(\mathbf{y}))^2 \int_0^1 f''(\bar{g}(\mathbf{y}) + s\Delta g_M(\mathbf{y})) (1-s) ds \middle| \mathbf{y} \right] \right], \end{aligned}$$

because the inner randomizations are independent. For the first term in (68),

$$(69) \quad \begin{aligned} \frac{2}{N} \mathbb{E} \left[\mathbb{V} \left[f'(\bar{g}(\mathbf{y}))\Delta g_M(\mathbf{y}) \middle| \mathbf{y} \right] \right] &= \frac{2}{N} \mathbb{E} \left[(f'(\bar{g}(\mathbf{y})))^2 \mathbb{V} \left[\Delta g_M(\mathbf{y}) \middle| \mathbf{y} \right] \right], \\ &\leq \frac{2}{N} \mathbb{E} \left[(f'(\bar{g}(\mathbf{y})))^2 \mathbb{E} \left[|\Delta g_M(\mathbf{y})|^2 \middle| \mathbf{y} \right] \right], \\ &\leq \frac{2}{N} \mathbb{E} \left[(f'(\bar{g}(\mathbf{y})))^2 |\bar{g}(\mathbf{y})|^2 \right] k^2 C_{\epsilon, d_2}^2 M^{-2+2\epsilon}, \end{aligned}$$

by Assumption 6 and the Koksma–Hlawka inequality (8). Using Hölder's inequality,

$$(70) \quad \begin{aligned} \frac{2}{N} \mathbb{E} \left[(f'(\bar{g}(\mathbf{y})))^2 |\bar{g}(\mathbf{y})|^2 \right] k^2 C_{\epsilon, d_2}^2 M^{-2+2\epsilon} &\leq \frac{2}{N} \mathbb{E} \left[(f'(\bar{g}(\mathbf{y})))^{2p} \right]^{\frac{1}{p}} \mathbb{E} \left[|\bar{g}(\mathbf{y})|^{2q} \right]^{\frac{1}{q}} k^2 C_{\epsilon, d_2}^2 M^{-2+2\epsilon}, \\ &< \infty, \end{aligned}$$

by Assumptions 5 and 6. For the second term in (68), we have

$$\begin{aligned}
& \frac{2}{N} \mathbb{E} \left[\mathbb{V} \left[(\Delta g_M(\mathbf{y}))^2 \int_0^1 f''(\bar{g}(\mathbf{y}) + s\Delta g_M(\mathbf{y})) (1-s) ds \middle| \mathbf{y} \right] \right], \\
& \leq \frac{2}{N} \mathbb{E} \left[\mathbb{E} \left[\left| (\Delta g_M(\mathbf{y}))^2 \int_0^1 f''(\bar{g}(\mathbf{y}) + s\Delta g_M(\mathbf{y})) (1-s) ds \right|^2 \middle| \mathbf{y} \right] \right], \\
& \leq \frac{2}{N} \mathbb{E} \left[\mathbb{E} \left[|\Delta g_M(\mathbf{y})|^4 \left(\int_0^1 |f''(\bar{g}(\mathbf{y}) + s\Delta g_M(\mathbf{y}))| (1-s) ds \right)^2 \middle| \mathbf{y} \right] \right], \\
& \leq \frac{1}{2N} \mathbb{E} \left[\mathbb{E} \left[|\Delta g_M(\mathbf{y})|^4 \middle| \mathbf{y} \right] |f''(K\bar{g}(\mathbf{y}))|^2 \right], \\
(71) \quad & \leq \frac{1}{2N} \mathbb{E} \left[|\bar{g}(\mathbf{y})|^4 |f''(K\bar{g}(\mathbf{y}))|^2 \right] k^4 C_{\epsilon, d_2}^4 M^{-4+4\epsilon},
\end{aligned}$$

by Assumption 6 and the Koksma–Hlawka inequality (8) for any $\epsilon > 0$. Using Hölder's inequality, we have that

$$\begin{aligned}
(72) \quad & \frac{1}{2N} \mathbb{E} \left[|\bar{g}(\mathbf{y})|^4 |f''(K\bar{g}(\mathbf{y}))|^2 \right] k^4 C_{\epsilon, d_2}^4 M^{-4+4\epsilon} \leq \frac{1}{2N} \mathbb{E} \left[|\bar{g}(\mathbf{y})|^{4q} \right]^{\frac{1}{q}} \mathbb{E} \left[|f''(K\bar{g}(\mathbf{y}))|^{2p} \right]^{\frac{1}{p}} k^4 C_{\epsilon, d_2}^4 M^{-4+4\epsilon}, \\
& < \infty,
\end{aligned}$$

by Assumptions 5 and 6. □

Remark 6 (rQMC analysis for specific problems). *Detailed analyses of the performance of rQMC estimators for integrands based on specific finite element formulations are available (e.g., [55, 56, 44]). However, for the generality of the bias and variance bounds of the rQMC method, the assumptions are restricted to the differentiability and integrability of the integrands. Moreover, the dependence on the dimension d_2 can be neglected under appropriate regularity conditions (see Remark 5).*

Using Proposition 3 and 4, we analyzed the work required for the rDLQMC estimator in terms of the number of samples and the discretization parameter of the inner integrand to achieve a prescribed tolerance. First, we ensured that the rDLQMC error (36) is smaller than some tolerance $TOL > 0$; that is,

$$\begin{aligned}
(73) \quad & |I_{\text{rDLQ}} - I| \leq |\mathbb{E}[I_{\text{rDLQ}}] - I| + |I_{\text{rDLQ}} - \mathbb{E}[I_{\text{rDLQ}}]|, \\
& \leq |\mathbb{E}[I_{\text{rDLQ}}] - I| + C_\alpha \sqrt{\mathbb{V}[I_{\text{rDLQ}}]}, \quad \text{with probability } 1 - \alpha \\
& < TOL.
\end{aligned}$$

An error-splitting parameter $\kappa \in (0, 1)$ is introduced to control the bias and statistical error separately to obtain the following:

$$(74) \quad |\mathbb{E}[I_{\text{rDLQ}}] - I| \leq (1 - \kappa)TOL,$$

and

$$(75) \quad C_\alpha \sqrt{\mathbb{V}[I_{\text{rDLQ}}]} \leq \kappa TOL,$$

which is written as

$$(76) \quad \mathbb{V}[I_{\text{rDLQ}}] \leq \left(\frac{\kappa TOL}{C_\alpha} \right)^2.$$

Optimizing the error-splitting parameter κ enables balancing the number of inner and outer samples to control the total error (73) efficiently. Substituting the error bounds established in Propositions (3) and (4) yields the following sufficient conditions to meet the error criterion (73):

$$(77) \quad C_{\text{disc}} h^\eta + \frac{C_{\text{Q},3}}{M^{2-2\epsilon}} \leq (1 - \kappa)TOL,$$

and

$$(78) \quad \frac{C_{\text{Q},1}}{N^{2-2\epsilon-2 \max_i A_i}} + \frac{C_{\text{Q},2}}{NM^{2-2\epsilon}} \leq \left(\frac{\kappa TOL}{C_\alpha} \right)^2,$$

where the constant terms in the bounds for the bias and statistical error ((41) and (57)) are combined, neglecting higher-order terms.

Proposition 5 (Optimal work of the rDLQMC estimator). *Given Assumptions 1 to 6, assuming that $|f''|$ and $|f'''|$ are monotonic, the total work of the optimized rDLQMC estimator (33) for a specified error tolerance $TOL > 0$ is given by*

$$(79) \quad W_{rDLQ}^* = \mathcal{O} \left(TOL^{-\left(\frac{2}{2-2\epsilon-2\max_i A_i} + \frac{1}{2-2\epsilon} + \frac{\gamma}{\eta} \right)} \right)$$

for any $\epsilon > 0$, $A_i > 0$, $1 \leq i \leq d_1$, $\max_i A_i < 1/2$, and $h, \gamma > 0$, as $TOL \rightarrow 0$.

Proof. The computational work for the rDLQMC estimator with $R = S = 1$ is

$$(80) \quad W_{rDLQ} = \mathcal{O}(NMh^{-\gamma}).$$

We obtain the optimal rDLQMC estimator setting by minimizing the computational work (80) subject to the constraints (77) and (78); that is,

$$(81) \quad (N^*, M^*, h^*, \kappa^*) = \arg \min_{(N, M, h, \kappa)} NMh^{-\gamma} \quad \text{subject to} \quad \begin{cases} \frac{C_{Q,1}}{N^{2-2\epsilon-2\max_i A_i}} + \frac{C_{Q,2}}{NM^{2-2\epsilon}} \leq \left(\frac{\kappa TOL}{C_\alpha} \right)^2 \\ C_{\text{disc}} h^\eta + \frac{C_{Q,3}}{M^{2-2\epsilon}} \leq (1-\kappa)TOL \end{cases}.$$

This problem is solved using Lagrange multipliers to derive the optimal M^* and h^* in terms of κ and N . The equation for κ^* is cubic and has a closed-form solution, but it is unwieldy to state explicitly. The last remaining equation for N^* has no closed-form solution; therefore, a simplified version must be solved, and the convergence of the resulting solution to the true solution as $TOL \rightarrow 0$ must be demonstrated. The optimal values for M and h satisfy the following:

$$(82) \quad M^* = \left(\frac{C_{Q,2}}{N \left(\frac{\kappa TOL}{C_\alpha} \right)^2 - \frac{C_{Q,1}}{N^{1-2\epsilon-2\max_i A_i}}} \right)^{\frac{1}{2-2\epsilon}},$$

and

$$(83) \quad h^* = \left(\frac{(1-\kappa)TOL - \frac{C_{Q,3}}{C_{Q,2}} \left(N \left(\frac{\kappa TOL}{C_\alpha} \right)^2 - \frac{C_{Q,1}}{N^{1-2\epsilon-2\max_i A_i}} \right)}{C_{\text{disc}}} \right)^{1/\eta}.$$

Moreover, the optimal κ^* is given by the real root of

$$(84) \quad \begin{aligned} & \left[\frac{C_{Q,3}}{C_{Q,2}} \left(\frac{NTOL}{C_\alpha} \right)^2 (\eta + \gamma(2-2\epsilon)) \right] \kappa^{*3} + \left[NTOL \left(\eta + \frac{\gamma(2-2\epsilon)}{2} \right) \right] \kappa^{*2} \\ & - \left[N \left(\eta TOL + \frac{C_{Q,3}}{C_{Q,2}} \frac{C_{Q,1}}{N^{1-2\epsilon-2\max_i A_i}} (\eta + \gamma(2-2\epsilon)) \right) \right] \kappa^* - \frac{\gamma(2-2\epsilon)C_{Q,1}C_\alpha^2}{2N^{1-2\epsilon-2\max_i A_i}TOL} = 0. \end{aligned}$$

Finally, the solution to the following yields the optimal N^* :

$$(85) \quad \begin{aligned} 0 = & \left[\frac{C_{Q,3}}{C_{Q,2}} \left(\frac{\kappa TOL}{C_\alpha} \right)^2 \right] N^{3-2\epsilon-2\max_i A_i} - \left[TOL \left(1 - \kappa \left(1 + \frac{\gamma}{2\eta} \right) \right) \right] N^{2-2\epsilon-2\max_i A_i} - \frac{C_{Q,3}}{C_{Q,2}} C_{Q,1} N \\ & + \frac{\gamma C_\alpha^2 C_{Q,1} (1-2\epsilon-2\max_i A_i)}{2\eta \kappa TOL}. \end{aligned}$$

It immediately follows from (81) that such an N^* exists. The optimal discretization parameter h^* is assumed to be independent of the sampling method (e.g., MC or rQMC). The bias constraint (77) is split as follows:

$$(86) \quad C_{\text{disc}} h^{*\eta} \leq \frac{1}{2}(1-\kappa)TOL,$$

$$(87) \quad \frac{C_{Q,3}}{M^{*2-2\epsilon}} \leq \frac{1}{2}(1-\kappa)TOL,$$

to derive the asymptotic rates in terms of the tolerance (TOL), implying that

$$(88) \quad h^* \propto TOL^{\frac{1}{\eta}},$$

and

$$(89) \quad M^* \propto TOL^{-\frac{1}{2-2\epsilon}}.$$

Next, we demonstrate that $N \propto TOL^{-\frac{2}{2-2\epsilon-2\max_i A_i}}$. From the variance constraint (78), we obtain the following:

$$(90) \quad \left(\frac{\kappa TOL}{C_\alpha}\right)^2 N^{2-2\epsilon-2\max_i A_i} - (1-\kappa)TOLN^{1-2\epsilon-2\max_i A_i} = C_{Q,1}.$$

The term on the right-hand side of (90) is constant in TOL . The equation in (90) can be solved by ignoring the second term on the left-hand side, yielding the following approximate solution:

$$(91) \quad N \approx \left(\frac{C_\alpha^2 C_{Q,1}}{\kappa^2}\right)^{\frac{1}{2-2\epsilon-2\max_i A_i}} TOL^{-\frac{2}{2-2\epsilon-2\max_i A_i}}.$$

We assess whether the ignored term in (90) approaches zero as $TOL \rightarrow 0$ by inserting (91) to determine whether this approximation converges to the true solution. For this term, we have

$$(92) \quad \begin{aligned} (1-\kappa)TOLN^{1-2\epsilon-2\max_i A_i} &\approx (1-\kappa) \left(\frac{C_\alpha^2 C_{Q,1}}{\kappa^2}\right)^{\frac{1-2\epsilon-2\max_i A_i}{2-2\epsilon-2\max_i A_i}} TOL^{1-\frac{2-4\epsilon-4\max_i A_i}{2-2\epsilon-2\max_i A_i}}, \\ &= (1-\kappa) \left(\frac{C_\alpha^2 C_{Q,1}}{\kappa^2}\right)^{\frac{1-2\epsilon-2\max_i A_i}{2-2\epsilon-2\max_i A_i}} TOL^{\frac{2\epsilon+2\max_i A_i}{2-2\epsilon-2\max_i A_i}}, \end{aligned}$$

where, for the exponent of TOL , $0 < (2\epsilon + 2\max_i A_i)/(2 - 2\epsilon - 2\max_i A_i) < 1$ as $\epsilon \rightarrow 0$ because of the assumption that $\max_i A_i < 1/2$. Thus, this term approaches zero as $TOL \rightarrow 0$. In contrast, ignoring the first term in (90) results in the approximate solution $N \approx -(C_{Q,1}/(1-\kappa))^{1/(1-2\epsilon-2\max_i A_i)} TOL^{-1/(1-2\epsilon-2\max_i A_i)}$. With this solution, the first term in (90) has an exponent of TOL which is strictly negative; thus, it approaches negative infinity as $TOL \rightarrow 0$. \square

The constants $C_{Q,1}$, $C_{Q,2}$, and $C_{Q,3}$ introduced in (77) and (78) can be estimated using $S, R > 1$ randomizations. Rather than using the approximate solution (91), we can also solve the equation in (85) numerically. Splitting the bias constraint (77) more elaborately than in (86) and (87) (i.e., by a splitting parameter possibly different from $1/2$) might improve the near-optimality of the approximation (91).

Remark 7 (Effects of inner randomization on the outer rQMC convergence). *The effectiveness of the (r)QMC estimators compared to the MC estimators relies on the specific low-discrepancy structure of the samples used for the evaluation of the integrands. Introducing randomness in these samples jeopardizes this structure. Nesting rQMC estimators with independent randomizations of the inner samples for each outer sample effectively transforms the outer samples into MC samples. However, the proof of Proposition 5 demonstrates that the effectiveness of the outer rQMC estimation can be preserved asymptotically if the number of outer and inner samples is appropriately increased. To the best of our knowledge, this insight is novel and constitutes a significant deviation from the analysis of other estimators discussed in the literature.*

Remark 8 (Rounding optimal parameters for practical purposes). *Because of the properties of low-discrepancy sequences, rounding the optimal number of samples N^* and M^* up to the nearest power of two is beneficial.*

4. NUMERICAL RESULTS

This section demonstrates the effectiveness and applicability of the derived double-loop methods for two OED problems. In Bayesian OED [11], the aim is to maximize the EIG of an experiment, given by the expected Kullback–Leibler divergence [5, 6, 12, 14] of the posterior distribution of the parameters of interest θ with respect to their prior distribution. We assumed the following data model:

$$(93) \quad \mathbf{y}_i(\boldsymbol{\xi}) = \mathbf{G}(\boldsymbol{\theta}_t, \boldsymbol{\xi}) + \varepsilon_i, \quad 1 \leq i \leq N_e,$$

where $\mathbf{Y} = (\mathbf{y}_1, \dots, \mathbf{y}_{N_e}) \in \mathbb{R}^{d_y \times N_e}$ represents noisy data generated from the deterministic model $\mathbf{G} : \mathbb{R}^{d_\theta} \times \mathbb{R}^{d_\xi} \rightarrow \mathbb{R}^{d_y}$ (evaluated at the true parameter vector $\boldsymbol{\theta}_t \in \mathbb{R}^{d_\theta}$) whose optimal design $\boldsymbol{\xi} \in \mathbb{R}^{d_\xi}$ we aim

to determine. Random observation noise is denoted by $\varepsilon_i \in \mathbb{R}^{d_y}$ for N_e available independent observations under a consistent experimental setup, where d_y, d_θ, d_ξ are positive integers. The noise ε_i is assumed to follow a centered normal distribution with a known covariance matrix $\Sigma_\varepsilon \in \mathbb{R}^{d_y \times d_y}$ independent of θ and ξ . The knowledge of the parameters of interest θ before experimenting is encompassed in the prior probability density function (PDF) $\pi(\theta)$. After the experiment, the knowledge is described by the posterior PDF of θ , given by Bayes' theorem as follows:

$$(94) \quad \pi(\theta|\mathbf{Y}, \xi) = \frac{p(\mathbf{Y}|\theta, \xi)\pi(\theta)}{p(\mathbf{Y}|\xi)},$$

where

$$(95) \quad p(\mathbf{Y}|\theta, \xi) := \det(2\pi\Sigma_\varepsilon)^{-\frac{N_e}{2}} \exp\left(-\frac{1}{2} \sum_{i=1}^{N_e} \mathbf{r}(\mathbf{y}_i, \theta, \xi) \cdot \Sigma_\varepsilon^{-1} \mathbf{r}(\mathbf{y}_i, \theta, \xi)\right)$$

represents the likelihood function. The data residual is given by (93) as follows:

$$(96) \quad \mathbf{r}(\mathbf{y}_i, \theta, \xi) := \mathbf{y}_i(\xi) - \mathbf{G}(\theta, \xi), \quad 1 \leq i \leq N_e.$$

We omitted the design parameter ξ for simplicity and distinguished between π for the PDFs of the parameters of interest and p for the PDFs of the data. The amount of information regarding θ gained from the experiment is given by

$$(97) \quad EIG := \int_{\mathcal{Y}} \int_{\Theta} \log\left(\frac{\pi(\theta|\mathbf{Y})}{\pi(\theta)}\right) \pi(\theta|\mathbf{Y}) d\theta p(\mathbf{Y}) d\mathbf{Y},$$

which is rewritten in terms of the likelihood function and the prior using Bayes' theorem and marginalization:

$$(98) \quad \begin{aligned} EIG &= \int_{\Theta} \int_{\mathcal{Y}} \log\left(\frac{p(\mathbf{Y}|\theta)}{\int_{\Theta} p(\mathbf{Y}|\vartheta)\pi(\vartheta) d\vartheta}\right) p(\mathbf{Y}|\theta) d\mathbf{Y} \pi(\theta) d\theta, \\ &= \int_{\Theta} \int_{\mathcal{Y}} \log(p(\mathbf{Y}|\theta)) p(\mathbf{Y}|\theta) d\mathbf{Y} \pi(\theta) d\theta - \int_{\Theta} \int_{\mathcal{Y}} \log\left(\int_{\Theta} p(\mathbf{Y}|\vartheta)\pi(\vartheta) d\vartheta\right) p(\mathbf{Y}|\theta) d\mathbf{Y} \pi(\theta) d\theta, \end{aligned}$$

where ϑ indicates a dummy variable for integration. The second term in (98) forms a nested integration problem to which the rDLQMC estimator is applied. Specifically, in this setting, the nonlinear outer function f in (20) is the logarithm, and the inner function g is the likelihood function.

Remark 9 (Closed-form expression for the first term in the EIG). *From (96), the likelihood in the logarithm in the first term of (98) depends only on ε_i , where $1 \leq i \leq N_e$, and can be computed in closed form for $\varepsilon_i \sim \mathcal{N}(\mathbf{0}, \Sigma_\varepsilon)$, where Σ_ε is a positive definite diagonal matrix in $\mathbb{R}^{d_y \times d_y}$ with entry $\sigma_{\varepsilon\{j,j\}}^2$, where $1 \leq j \leq d_y$. The solution to this integration problem in (98) is given by*

$$(99) \quad -\frac{N_e}{2} \sum_{j=1}^{d_y} \left(\log\left(2\pi\sigma_{\varepsilon\{j,j\}}^2\right) + 1\right).$$

A similar result is presented in [20]. Appendix B provides a derivation for completeness.

Furthermore, we constructed an importance sampling distribution for ϑ to reduce the variance of the (r)QMC methods further based on the Laplace approximation [7, 8, 9, 2, 3, 10, 13, 15, 16, 17, 18] (for a thorough discussion of the Bayesian OED formulation, see [7, 2, 4]). The Laplace approximation of the posterior is given by

$$(100) \quad \tilde{\pi}(\theta|\mathbf{Y}) = \frac{1}{\det(2\pi\Sigma)^{\frac{1}{2}}} \exp\left(-\frac{(\theta - \hat{\theta}) \cdot \Sigma^{-1}(\hat{\theta})(\theta - \hat{\theta})}{2}\right),$$

where

$$(101) \quad \hat{\theta} := \arg \min_{\theta \in \mathbb{R}^{d_\theta}} \left[\frac{1}{2} \sum_{i=1}^{N_e} \mathbf{r}(\mathbf{y}_i, \theta, \xi) \cdot \Sigma_\varepsilon^{-1} \mathbf{r}(\mathbf{y}_i, \theta, \xi) - \log(\pi(\theta)) \right]$$

represents the maximum a posteriori (MAP) estimate and

$$(102) \quad \Sigma^{-1}(\hat{\theta}) := N_e \nabla_{\theta} \mathbf{G}(\hat{\theta}, \xi) \cdot \Sigma_\varepsilon^{-1} \nabla_{\theta} \mathbf{G}(\hat{\theta}, \xi) - \nabla_{\theta} \nabla_{\theta} \log(\pi(\hat{\theta}))$$

provides the approximate negative inverse Hessian of the log-likelihood evaluated at the MAP. The Laplace approximation error increases for an increasingly nonlinear \mathbf{G} [36]. Changing the measure for the inner integral in (98) to the approximate posterior (100) provides the DLMC estimator with importance sampling (DLMCIS; introduced in [2]) and novel rDLQMC estimator with importance sampling (rDLQMCIS):

$$(103) \quad I_{\text{rDLQIS}} := \frac{1}{N} \sum_{n=1}^N \log \left(\frac{1}{M} \sum_{m=1}^M p(\mathbf{Y}^{(n)} | \boldsymbol{\vartheta}^{(n,m)}) \frac{\pi(\boldsymbol{\vartheta}^{(n,m)})}{\tilde{\pi}(\boldsymbol{\vartheta}^{(n,m)} | \mathbf{Y}^{(n)})} \right),$$

where $\boldsymbol{\vartheta}^{(n,m)}$ is now distributed according to $\tilde{\pi}(\cdot | \mathbf{Y}^{(n)})$ rather than $\pi(\cdot)$, where $1 \leq n \leq N$ and $1 \leq m \leq M$.

The EIG can be estimated using (103) in combination with the expression in (99). Laplace-based importance sampling can significantly reduce the number of required inner samples for both estimators. To construct the rDLQMCIS estimator, we followed the steps in [7] and [2], replacing MC samples with rQMC samples. Combining importance sampling with rQMC is notably more complex from a theoretical perspective than combining importance sampling with MC. The effects of Laplace-based importance sampling on the rQMC convergence rate for a standard normal prior were analyzed in [45]. Specifically, if at least one eigenvalue of the matrix (102) is smaller than 1, the condition in Assumption 1 can no longer be guaranteed. Finding a more suitable importance sampling scheme (see [45, 46]) is not the focus of the current theoretical work and is left for future research. Laplace-based importance sampling for a uniform prior introduces a discontinuity, as the uniform distribution has compact support. Discontinuities in the integrand lead to unbounded Hardy–Krause variation, complicating the application of rQMC methods. The work [62] proposed an acceptance–rejection algorithm to generate appropriate MC samples. However, rejecting samples jeopardizes the low-discrepancy structure of rQMC samples.

The interplay between Laplace-based importance sampling and the QMC method for rank-1 lattice rules was analyzed in [9]. Without importance sampling, the inner integral approximation can produce numerical underflow [2] unless a vast number of inner samples is used, rendering these methods impractical in those cases.

Remark 10 (Uniqueness of the MAP). *The posterior distribution of the parameters of interest in Bayesian OED problems is often highly concentrated around a unique maximum [2]. However, even if the posterior is multimodal, recurring use of the Laplace approximation can still produce helpful importance sampling distributions [61]. Another approach was followed in [64], where a global search, using distinct starting values, for multiple maxima of the posterior distribution was conducted. The Hessian was subsequently approximated at the resulting maxima to construct a mixture distribution for importance sampling in EIG estimation.*

Alternatively, we could estimate the EIG using a single-loop (rQ)-MC method by approximating the posterior in (97) using (100). In this case, no nested integration is necessary, and the EIG is estimated as follows:

$$(104) \quad EIG \approx \int_{\boldsymbol{\Theta}} \left[\frac{1}{2} \log(\det(2\pi\boldsymbol{\Sigma}(\boldsymbol{\theta}))) - \frac{d_{\boldsymbol{\theta}}}{2} - \log(\pi(\boldsymbol{\theta})) \right] \pi(\boldsymbol{\theta}) d\boldsymbol{\theta}.$$

This approach leads to the MC Laplace (MCLA) estimator (introduced in [7]) and the rQMC Laplace (rQMCLA) estimator based on (104):

$$(105) \quad I_{\text{rQLA}} := \frac{1}{N} \sum_{n=1}^N \left[\frac{1}{2} \log(\det(2\pi\boldsymbol{\Sigma}(\boldsymbol{\theta}^{(n)}))) - \frac{d_{\boldsymbol{\theta}}}{2} - \log(\pi(\boldsymbol{\theta}^{(n)})) \right],$$

both of which have a bias of $\mathcal{O}_{\mathbb{P}}\left(\frac{1}{N_e}\right)$.² The MCLA estimator uses MC points, whereas the rQMCLA estimator uses rQMC points. For both estimators, we replaced the MAP with samples from the prior (see [7, 2] for details).

The rQMC rates in (77) and (78) are typically not observed in practice for finite N and M . Furthermore, obtaining the constants $C_{\text{Q},1}$, $C_{\text{Q},2}$, and $C_{\text{Q},3}$ is challenging; hence, the constraints on the bias and statistical

²The notation $X_M = \mathcal{O}_{\mathbb{P}}(C_M)$ for a sequence of random variables X_M and constants C_M is specified as follows. For any $\epsilon > 0$, there exists finite $K(\epsilon), M_0 > 0$ such that $\mathbb{P}(|X_M| > K(\epsilon) | C_M) < \epsilon$ holds for all $M \geq M_0$.

error are restated as follows:

$$(106) \quad C_{\text{disc}}h^\eta + \frac{C_{\text{Q},3}}{M^{1+\delta}} \leq (1 - \kappa)TOL,$$

and

$$(107) \quad \frac{C_{\text{Q},1}}{N^{1+\beta}} + \frac{C_{\text{Q},2}}{NM^{1+\delta}} \leq \left(\frac{\kappa TOL}{C_\alpha} \right)^2,$$

respectively, where $0 < \beta, \delta < 1$, correspond to the observed improvement of the rQMC convergence over the MC convergence. We estimated the constants $C_{\text{Q},1}$ and β using a pilot run of the rDLQMC estimator (30) with $S > 1$, $R = 1$ randomizations, and the constants $C_{\text{Q},2}, C_{\text{Q},3}$, and δ with a separate pilot run with $S = 1$, $R > 1$ randomizations. Moreover, the factor two appearing in (57), stemming from the bound (60) is a consequence of neglecting covariance terms. Ignoring this factor had negligible results in practice. Thus, in our computations, we replaced expression (57) by

$$(108) \quad \mathbb{V}[I_{\text{rDLQ}}] \lesssim \frac{b^2 B_A^2 C_{\epsilon, d_1}^2}{N^{2-2\epsilon-2\max_i A_i}} + \frac{\mathbb{E}[|\bar{g}_h|^2 |f'(\bar{g}_h)|^2] k^2 C_{\epsilon, d_2}^2}{NM^{2-2\epsilon}} + \frac{\mathbb{E}[|\bar{g}_h|^4 |f''(K\bar{g}_h)|^2] (\Gamma_{d_1} + 1) k^4 C_{\epsilon, d_2}^4}{4NM^{4-4\epsilon}}.$$

In Appendix C, we derived the condition that the data model \mathbf{G} applied to the inverse CDF of the parameters of interest must be uniformly Lipschitz continuous and have bounded mixed derivatives for Proposition 1 to guarantee good rQMC convergence rates for the EIG. In Appendix D, we verified Condition (40) for the observation noise distributed according to a truncated normal distribution and demonstrated weak dependence of the constant

$$(109) \quad k = \mathcal{O}\left(\log(TOL^{-1})^{\frac{1}{2}}\right)$$

in Condition (40) on TOL . The additional error introduced by this truncation was also bounded in Appendix D as $o(TOL)$ for observation noise distributed according to a normal distribution. In Corollary 1, the total error of the rDLQMC estimator applied to estimate the EIG for observation noise from a standard normal distribution is presented, specifying the dependence of the bounds on the bias and statistical error on the error tolerance TOL introduced via k in (109). The verification of the Lipschitz condition for specific data models is left for future research. We applied the confidence constant $C_\alpha = \Phi^{-1}(1 - \alpha/2)$ implied by the CLT in the numerical examples. A more cautious approach could be taken, where $C_\alpha = 1/\sqrt{\alpha}$, as implied by the Chebyshev inequality. The investigation of the applicability of the CLT for rQMC is the subject of current research [50].

4.1. Example 1: Pharmacokinetics example with exact sampling. We replicated the results of the numerical experiment in [53, Example 4.2.] to underscore the applicability and cost-effectiveness of the proposed algorithms. Pharmacokinetic experiments aim to determine patient-specific parameters in a medical setting. We followed [53], where a simplified version of [57] was employed. A drug is administered to a patient at time $t_0 = 0$, and 15 measurements of the drug concentration are taken via blood samples at times (t_1, \dots, t_{15}) , where $t_0 < t_1 < \dots < t_{15} < 24$ over the next 24 h. The sampling times represent the experimental design, and $(\xi_1, \dots, \xi_{15}) := (t_1, \dots, t_{15})$, and $d_\xi = d_y = 15$. Only one sample is assumed to be taken at a time (i.e., $N_e = 1$). The data observations on the drug concentration are modeled in (93), where

$$(110) \quad G_j(\boldsymbol{\theta}, \boldsymbol{\xi}) := \frac{D}{\theta_3} \frac{\theta_1}{\theta_1 - \theta_2} (e^{-\theta_2 \xi_j} - e^{-\theta_1 \xi_j}), \quad 1 \leq j \leq 15,$$

and $\boldsymbol{\varepsilon} \sim \mathcal{N}(\mathbf{0}, 10^{-2} \mathbf{I}_{d_y \times d_y})$, denotes the observation noise, $D = 400$ represents the dose administered at ξ_0 , and $\boldsymbol{\theta} = (\theta_1, \theta_2, \theta_3) \in \mathbb{R}^{d_\theta}$, where $d_\theta = 3$, represents the parameters of interest. The prior consists of independent components with $\log(\theta_1) \sim \mathcal{N}(0, 0.05)$, the first-order absorption constant, $\log(\theta_2) \sim \mathcal{N}(\log(0.1), 0.05)$, the first-order elimination constant, and $\log(\theta_3) \sim \mathcal{N}(\log(20), 0.05)$, the volume of distribution. The full model includes a multiplicative error term, which is neglected in the simplified version. Further, the function \mathbf{G} can be evaluated without additional discretization (i.e., $C_{\text{disc}} = 0$ in (106)). Following [53] and [57], we compared two design choices, $\xi_j^{\text{geom}} = 0.94 \times 1.25^{j-1}$ and $\xi_j^{\text{even}} = 0.3 + 1.6 \times (j - 1)$. Another design was presented in [53] and [57] based on the Beta distribution; however, the information was insufficient to replicate those results.

Figure 1 presents the optimal work required to estimate the EIG with a prescribed tolerance (TOL) for $\boldsymbol{\xi}^{\text{geom}}$. The constants $C_{\text{Q},1}$ and β were estimated using $N = 2048$ and $M = 4$ samples and $S = 32$ and $R = 1$

randomizations. The constants $C_{Q,2}$, $C_{Q,3}$, and δ were estimated using $N = 4$ and $M = 2048$ samples and $S = 1$ and $R = 32$ randomizations. The constants for the DLMCIS estimator were estimated in one pilot run using $N = M = 2028$ samples. We used $N = 64$ and $M = 131,072$ samples for the DLMC estimator to avoid numerical underflow. The rDLQMC estimator without importance sampling still suffered from numerical underflow, even with numerous inner samples. The constants for the MCLA estimator were estimated using $N = 2048$ samples, and the constants for the rMCQLA estimator were estimated using $N = 2048$ samples and 32 randomizations. The rDLQMCIS result was applied as a reference to estimate the bias of the MCLA and rQMCLA estimators.

In Figure 1, as the latter two estimators approach the inherent bias from the Laplace approximation, their computational work rapidly increases. However, for high and intermediate tolerances, rQMCLA is highly efficient as $\beta \approx 0.86$, yielding a convergence rate of $2/(1+\beta) \approx 1.08$. The rDLQMCIS estimator is competitive for any tolerance, as $\beta \approx 0.71$ and $\delta \approx 0.78$, generating a convergence rate of $2/(1+\beta) + 1/(1+\delta) \approx 1.73$. This observed convergence rate is substantially better than the theoretically optimal rate of 2 for the MLMC estimators with or without inner rQMC sampling [19, 21]. The MLMC estimator with outer rQMC sampling [23] or outer and inner rQMC sampling could generate a better convergence rate; however, the error analysis for these estimators is considerably more complicated. Thus, it is not the subject of this work.

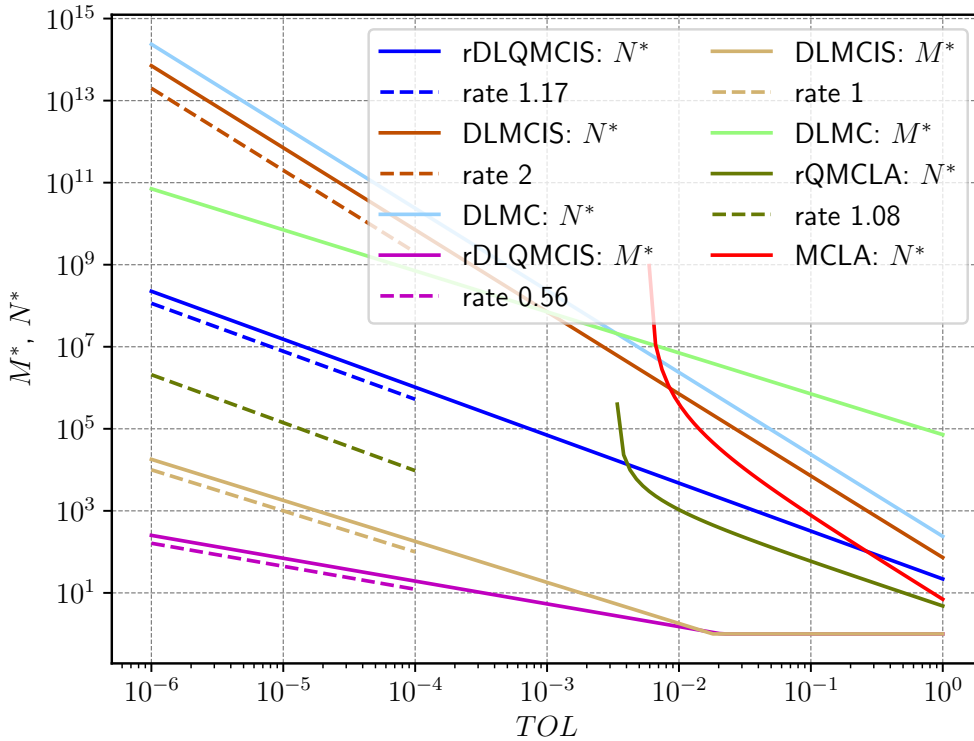


FIGURE 1. Example 1: Optimal number of the outer (N^*) and inner (M^*) samples vs. tolerance (TOL) for the rDLQMCIS, DLMCIS, DLMC, rQMCLA, and MCLA estimators. Only one inner sample is required for high tolerances in the rDLQMCIS and DLMCIS estimators due to importance sampling. Hence, the projected rate is attained only for low tolerances. No inner sampling is necessary for the rQMCLA and MCLA estimators; however, these estimators have bias due to the Laplace approximation relative to the number of experiments. As the tolerance approaches this bias, the required number of samples and hence the estimator cost exceed all bounds.

Figure 2 demonstrates the optimal work for the rDLQMCIS, DLQMCIS, DLMC, rQMCLA, and MCLA estimators. Although the latter two are highly efficient, the inherent bias from the Laplace approximation renders them ineffective for low tolerances.

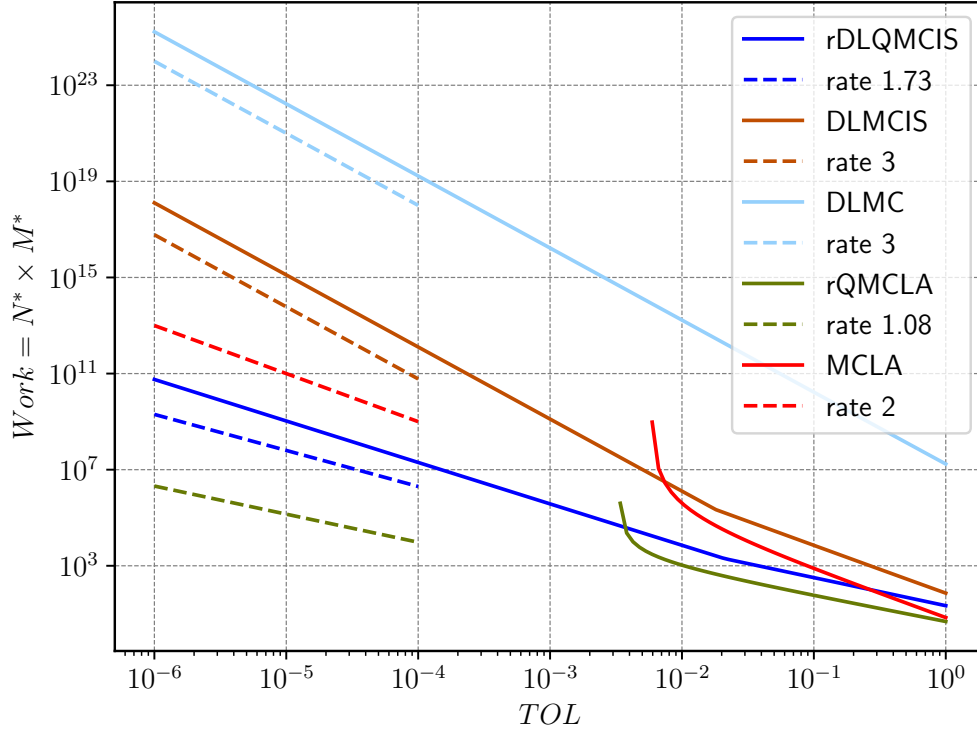


FIGURE 2. Example 1: Optimal work ($N^* \times M^*$) vs. tolerance (TOL) for the rDLQMCIS, DLQMCIS, DLMC, rQMCLA, and MCLA estimators. Only one inner sample is necessary for high tolerances due to importance sampling for the rDLQMCIS and the DLQMCIS estimators. Hence, the projected rate is attained only for low tolerances. The rQMCLA and MCLA estimators require only outer sampling.

Table 1 compares the MLMC algorithm proposed in [53] and the rDLQMCIS estimator. The EIG is estimated for a prescribed tolerance $TOL = 5 \cdot 10^{-4}$ for the two designs ξ^{geom} and ξ^{even} . Our results match theirs to the provided accuracy. The preasymptotic computational cost of the rDLQMCIS estimator, indicated as $N^*(M^* + 1)$, not considering the cost to obtain the Laplace approximation, increases at a rate of 1.73 for ξ^{geom} and 1.65 for ξ^{even} . Although this is lower than the rate of 2 for the MLMC estimator, due to the properties of low-discrepancy point sets, the number of samples must be rounded up to a power of 2, leading to a slightly higher cost for ξ^{geom} . This finding implies that our results are accurate up to an even higher tolerance.

ξ	MLMC cost [53]	rDLQMCIS cost	MLMC EIG [53]	rDLQMCIS EIG	MLMC rate [53]	rDLQMCIS rate
geom	$1.85 \cdot 10^7$	$2.4 \cdot 10^7$	10.74	10.7372	2	1.73
even	$1.91 \cdot 10^7$	$1.2 \cdot 10^7$	10.21	10.2065	2	1.65

TABLE 1. Example 1: Cost and accuracy comparison of the MLMC [53] and rDLQMCIS estimators for $TOL = 5 \cdot 10^{-4}$. The number of samples must be a power of 2 for the low-discrepancy sequences used; thus, the cost for a certain tolerance may be increased by a constant factor.

4.2. Example 2: Thermo-mechanics example with inexact sampling. In this example, \mathbf{G} is the solution operator of the PDE described below; therefore, we applied an appropriate finite element approximation \mathbf{G}_h . The domain is given by $\mathcal{D} = [0, 1]^2 \setminus \mathcal{B}$, where \mathcal{B} is a ball centered at $\mathbf{0}$ with a radius of 0.1. The problem is time-dependent, with observations occurring in $t \in [0, T]$. We solved the following problem for the unknown absolute temperature ϑ (not to be confused with the dummy variable presented in (95)) and unknown displacement \mathbf{u} for fully coupled thermomechanical fields (for more information and a staggered algorithm, see [40]).

A weak form of the heat equation is given as follows:

$$(111) \quad \int_{\mathcal{D}} \rho \vartheta_0 \dot{s} \hat{\vartheta} \, d\mathcal{D} - \int_{\mathcal{D}} \mathbf{q} \cdot \nabla \hat{\vartheta} \, d\mathcal{D} = - \int_{\partial\mathcal{D}} \mathbf{q} \cdot \mathbf{n} \hat{\vartheta} \, dS \quad \forall \hat{\vartheta} \in V_{\vartheta},$$

where

$$(112) \quad \rho \vartheta_0 \dot{s} = \rho \theta_2 \dot{\vartheta} + \theta_1 (3\lambda + 2\mu) \vartheta_0 \operatorname{tr}(\dot{\mathbf{e}}),$$

and

$$(113) \quad \mathbf{q} = -\theta_3 \nabla \vartheta.$$

The parameters of interest are $\boldsymbol{\theta} = (\theta_1, \theta_2, \theta_3) \in \Theta \subset \mathbb{R}^3$; θ_1 , the thermal expansion coefficient; θ_2 , the specific heat per unit volume at constant strain; and θ_3 , the thermal conductivity. Furthermore, the fixed parameters are the material density $\rho = 2700 \text{kg/m}^3$, entropy per unit of mass in the current s , Lamé constants $\lambda = 7000/1.56$ and $\mu = 35000/1.3$, and initial temperature $\vartheta_0 = 293 \text{K}$. Finally, the strain tensor $\mathbf{e} = \nabla^s \mathbf{u}$, the symmetric part of the gradient of \mathbf{u} ,

$$(114) \quad \nabla^s \mathbf{u} = \frac{1}{2} (\nabla \mathbf{u} + (\nabla \mathbf{u})^\top),$$

the unit outward normal \mathbf{n} , and the function space for the temperature field V_{ϑ} for all $t \in [0, T]$ were also assessed. For the time derivatives, the implicit Euler scheme with a log-spaced step size was applied. A weak form of the momentum equation is

$$(115) \quad \int_{\mathcal{D}} (\lambda \operatorname{tr}(\mathbf{e}) \mathbf{1} + 2\mu \mathbf{e} - \theta_1 (3\lambda + 2\mu) (\vartheta - \vartheta_0) \mathbf{1}) : \nabla_s \hat{\mathbf{u}} \, d\mathcal{D} = W_{\text{ext}}(\hat{\mathbf{u}}) \quad \forall \hat{\mathbf{u}} \in V_U,$$

where V_U denotes the function space for the displacement, $\mathbf{1}$ indicates the identity tensor, and W_{ext} represents the linear functional corresponding to the work of body external forces (neglecting inertia effects; thus, a quasi-static but transient model) and surface tractions on the boundary. The unknown absolute temperature ϑ was replaced with the temperature variation $\Delta = \vartheta - \vartheta_0$. For this experiment, a temperature increase of $\Delta = 10^\circ \text{C}$ was applied at the circular exclusion. Stress and flux-free conditions were applied at the remaining boundaries, and symmetry conditions were applied on the corresponding symmetry planes (for details on the FEM, see Appendix G).

The discretization parameter h affects the problem formulation as follows. The mesh-resolution parameter h_{mesh} of the FEM was set to $h_{\text{mesh}} = \lceil 1/h \rceil$, where $\lceil \cdot \rceil$ is the ceiling operator. Furthermore, the number of time steps was set to $h_{\text{time}} = \lceil 1/h^2 \rceil$, because the solution to the heat equation (111) depends linearly on time and quadratically on space. Decoupling the parameters h_{mesh} and h_{time} would enable using multi-index MC techniques [41]. The actual observation times were selected on a log scale because the problem can be stiff initially. In addition, as the problem approaches a steady state, the observations become increasingly similar, leading to numerical issues unless the observation times are sufficiently spread apart.

The following mutually independent prior distributions were assumed for the parameters of interest (θ):

$$(116) \quad \theta_1 \sim \mathcal{U}(1.81, 2.81) \times 10^{-5}, \quad \theta_2 \sim \mathcal{U}(8.6, 9.6) \times 10^{-4}, \quad \theta_3 \sim \mathcal{U}(1.87, 2.87) \times 10^{-4}.$$

For the observation noise, we assumed that $\varepsilon_i \sim \mathcal{N}(\mathbf{0}, \Sigma_\varepsilon)$, where $1 \leq i \leq N_e$. Moreover, Σ_ε represents a diagonal matrix in $\mathbb{R}^{d_y \times d_y}$, where the first $d_y/2$ diagonal entries corresponding to the strain measurements are $\sigma_{\varepsilon,1}^2 = 10^{-10}$, and the second $d_y/2$ diagonal entries corresponding to the measurements of the increase in temperature are denoted by $\sigma_{\varepsilon,2}^2 = 1/4$. The data model, as presented in (93), is as follows:

$$(117) \quad \mathbf{y}_i(\boldsymbol{\xi}) = \mathbf{G}_h(\boldsymbol{\theta}_t, \boldsymbol{\xi}) + \varepsilon_i, \quad 1 \leq i \leq N_e.$$

We considered two measurements of the strain and two measurements of the temperature increase at three observation times each, yielding $d_y = 12$ observations. For $N_e = 1$ experiment, the outer integration in (98) is $N_e \times d_y + d_\theta = 15$ dimensional, and the inner integration is $d_\theta = 3$ dimensional. Figure 3 presents the domain \mathcal{D} , and a circular exclusion occurs in the lower left corner. For the design parameter $\boldsymbol{\xi} = (\xi_1, \xi_2)$, ξ_1 represents the position of the sensors, and ξ_2 indicates the maximum observation time. The sensors for the strain are located at $(0.0 + \xi_1, 1.0)$ and $(0.6 + \xi_1, 1.0)$. The sensors for the temperature increase are located at $(0.2 + \xi_1, 1.0)$ and $(0.4 + \xi_1, 1.0)$, where $\xi_1 \in \{0.0, 0.2, 0.4\}$. Figure 4 depicts the temperature increase at the observation times $t = \{10^3, 10^4\}$ for $\xi_1 = 0.2$.

Figure 5 presents the number of required optimal samples for the rDLQMC and DLMC estimators obtained through pilot runs using $N, M = 128$ samples and $S = 8$ and $R = 1$ randomizations for the constants $C_{Q,1}$ and β for the rDLQMC estimator, and $N, M = 128$ samples and $S = 1$ and $R = 8$ randomizations for the constants $C_{Q,2}, C_{Q,3}$ and δ . Moreover, for the pilot run of DLMC, $N = M = 256$ samples were applied. The resulting rates for rDLQMC were $\beta = 0.6$ and $\delta = 0.46$. Hence, N^* increases at a rate of $2/(1 + \beta) \approx 1.25$ rather than a rate of 2, and M^* increases at a rate of $1/(1 + \delta) \approx 0.69$ rather than a rate of 1. Although these rates are worse than those for the previous example, they still reveal that the regularity in the physical model can be exploited and that using rQMC instead of MC is beneficial. As the allowed tolerance (TOL) approaches the bias from the Laplace approximation, the optimal splitting parameter κ^* is almost constant for the rDLQMC and DLMC estimators. The bias from the inner integration can be reduced by increasing the number of inner samples in both estimators (Figure 6). For this application, the reduction in variance was more pronounced compared to the reduction in bias; hence, κ^* was slightly smaller for the rDLQMC estimator than for the DLMC estimator, indicating that relatively more effort was required for bounding the bias error. Figure 7 depicts the optimal work given by $N^* \times M^* \times h^{*\gamma}$. A problematic measure concentration leading to numerical underflow was not observed for this example; thus, the rDLQMC and DLMC methods could be applied.

The EIG for the model in (117) is illustrated in Figure 8, where the experiment is evaluated for various sensor placements ξ_1 at observation times $t = \{4000, 10^{\frac{\log(4000) + \log(\xi_2)}{2}}, \xi_2\}$, $\xi_1 \in \{0.0, 0.2, 0.4\}$, and $\xi_2 \in \{2 \times 10^5, 4 \times 10^5, 6 \times 10^5, 8 \times 10^5\}$. The sensors require time to gain sufficient information; thus, the first observation time is fixed. Eventually, the process converges to a steady state, so the experiment must be terminated before $\xi_2 = 10^6$. The highest EIG was attained for $\xi_1 = 0.4$, where the sensors are farthest away from the source in the lower left corner at the optimal observation time $\xi_2 = 8 \times 10^5$. The rDLQMC estimator for the allowed error tolerance of $TOL = 0.2$ was used with only one randomization ($S, R = 1$) and N^*, M^* , and h^* from the pilots for the EIG approximation. This tolerance requires a discretization parameter $h \approx 0.13$. The choice of observation time had a greater effect on the EIG than the sensor selection, for which no clear preference was observed. Figure 9 illustrates the EIG for model (117) as a three-dimensional plot.

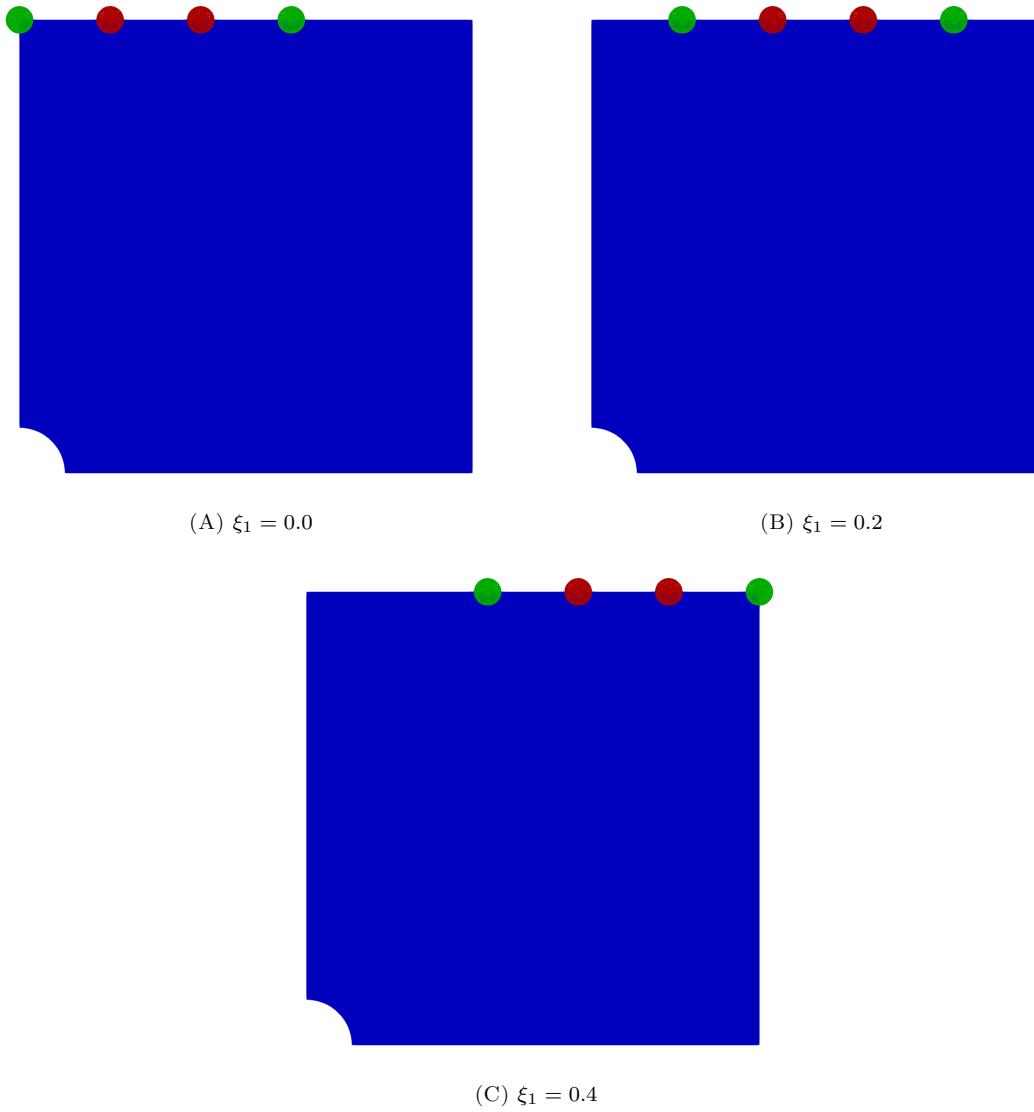


FIGURE 3. Example 2: Rectangular domain with the circular exclusion and sensor locations $\{(0.0 + \xi_1, 1.0), (0.2 + \xi_1, 1.0), (0.4 + \xi_1, 1.0), (0.6 + \xi_1, 1.0)\}$, where green indicates strain and red indicates temperature sensors).

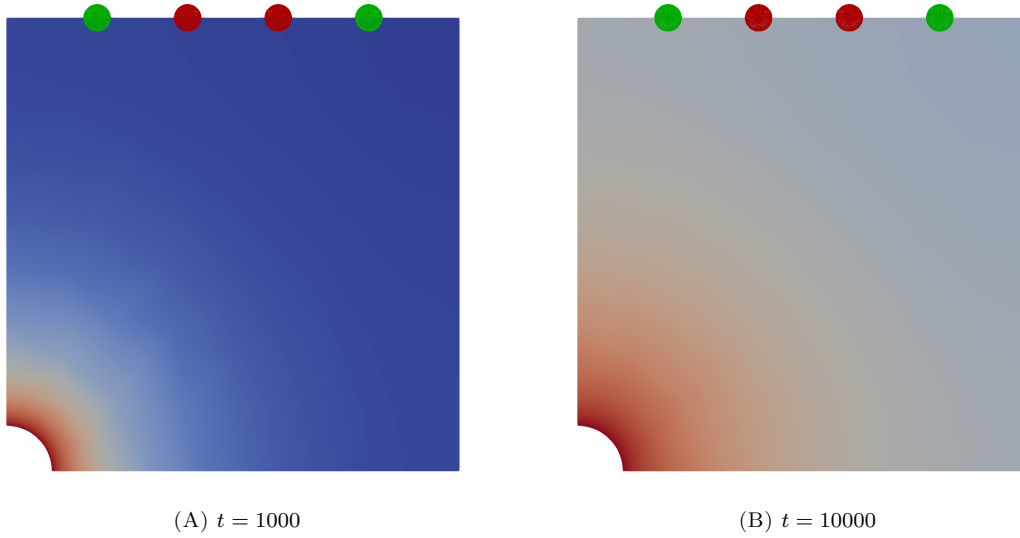


FIGURE 4. Example 2: Temperature increases at observation times of the experiment for the rectangular domain with a circular exclusion. Point-sensor locations are displayed as circles at the top of the domain.

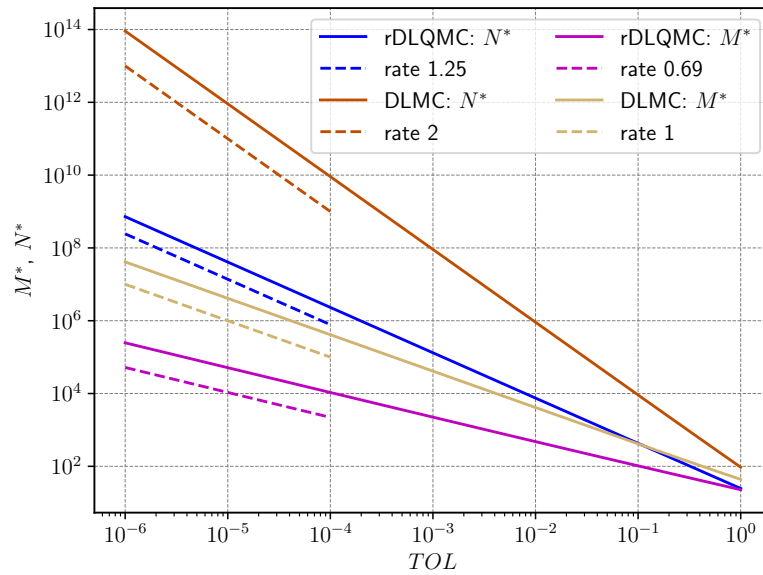


FIGURE 5. Example 2: Optimal number of the outer (N^*) and inner (M^*) samples vs. tolerance (TOL) for the rDLQMC and DLMC estimators.

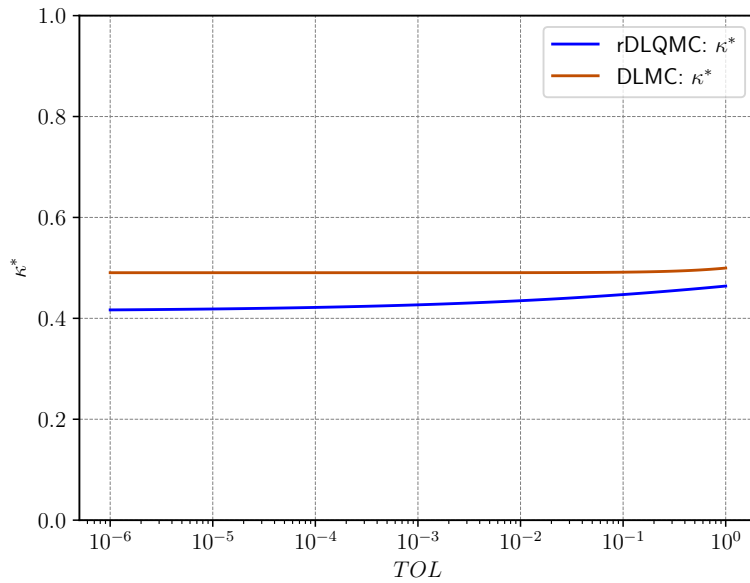


FIGURE 6. Example 2: Optimal splitting parameter (κ^*) vs. tolerance TOL for the rDLQMC, and DLMC estimators.

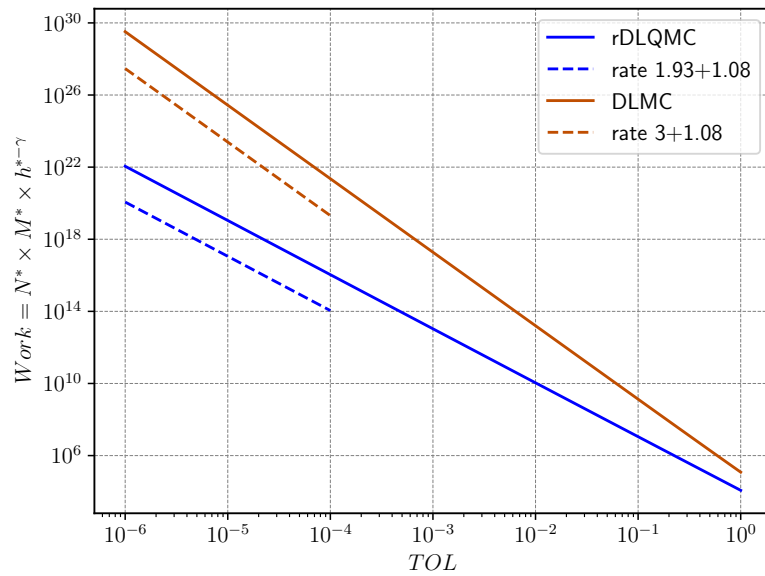


FIGURE 7. Example 2: Optimal work ($N^* \times M^* \times h^{*-\gamma}$) vs. tolerance TOL for the rDLQMC and DLMC estimators.

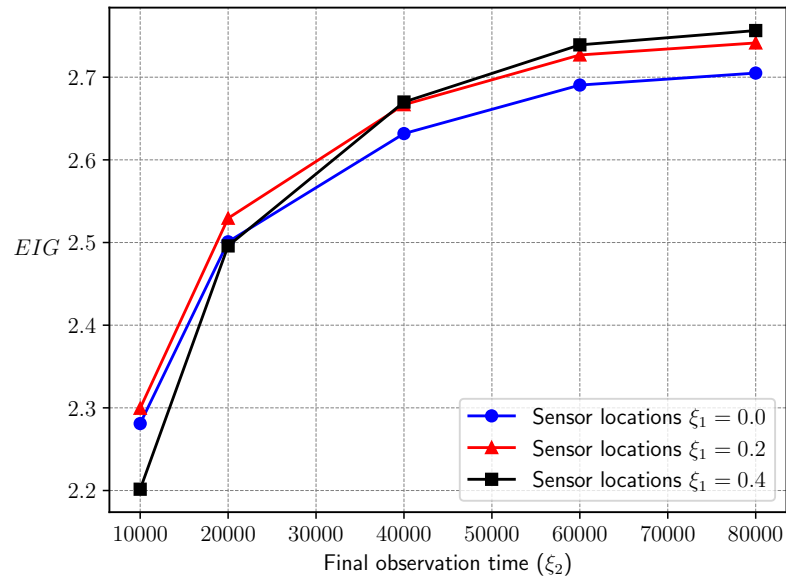


FIGURE 8. Example 2: Expected information gain (EIG) as a function of the design $\xi = (\xi_1, \xi_2)$, indicating sensor locations and observation times, estimated using the rDLQMC estimator with an allowed tolerance of $TOL = 0.2$. The maximum EIG is reached for $\xi_1 = 0.4$ and $\xi_2 = 8 \times 10^5$.

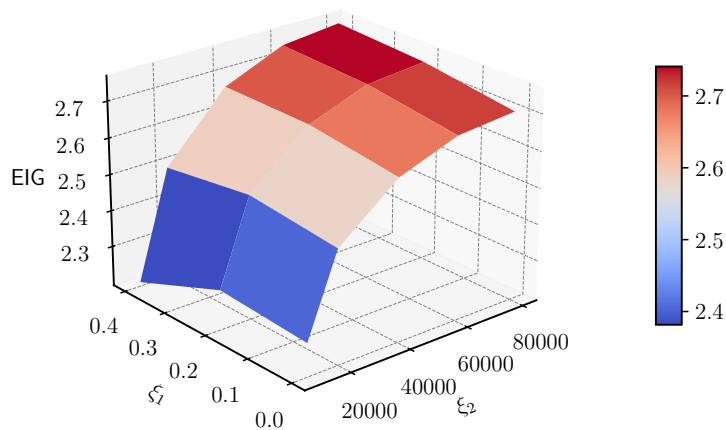


FIGURE 9. Example 2: Expected information gain (EIG) as a function of the design $\xi = (\xi_1, \xi_2)$, indicating sensor locations and observation times, estimated using the rDLQMC estimator with an allowed tolerance of $TOL = 0.2$. The maximum EIG is reached for $\xi_1 = 0.4$ and $\xi_2 = 8 \times 10^5$.

5. CONCLUSION

This paper proposes estimating nested integrals using randomized quasi-Monte Carlo (rQMC) approximations for outer and inner integrals, delivering the double-loop randomized quasi-Monte Carlo estimator (rDLQMC). For this method, we derived asymptotic error bounds and attained the near-optimal number of samples required for each approximation as the primary contribution of this work. The application to Bayesian optimal experimental design indicates that this method is superior to using the rQMC method for only one or neither integral approximation. Replacing the inner integral with the Laplace approximation yields an even more efficient estimator, but is only feasible for a high error tolerance. The numerical results of the combination of Laplace-based importance sampling with rQMC seem promising. Combining the multilevel MC (or the even more advanced multi-index MC) method with the rQMC method for the outer integral approximation leads to a more complicated error analysis, which is left for future work.

6. STATEMENTS AND DECLARATIONS

6.1. **Conflict of interest.** The authors have no conflicts to disclose.

6.2. **Data availability.** The data that support the findings of this study are available from the corresponding author upon reasonable request.

APPENDIX A. VARIANCE INEQUALITY

We derived the following inequality for the variance of the sum of (dependent) random variables $X^{(j)}$, where $1 \leq j \leq J$, possibly with different distributions, using the Cauchy–Schwarz inequality:

$$\begin{aligned}
\mathbb{V} \left[\sum_{j=1}^J X^{(j)} \right] &= \mathbb{E} \left[\left(\sum_{j=1}^J X^{(j)} - \mathbb{E} \left[\sum_{j=1}^J X^{(j)} \right] \right)^2 \right], \\
&= \mathbb{E} \left[\left(\sum_{j=1}^J X^{(j)} - \sum_{j=1}^J \mathbb{E} [X^{(j)}] \right)^2 \right], \\
&= \mathbb{E} \left[\left(\sum_{j=1}^J (X^{(j)} - \mathbb{E} [X^{(j)}]) \right)^2 \right], \\
&= \mathbb{E} \left[\left(\sum_{j=1}^J 1 \cdot (X^{(j)} - \mathbb{E} [X^{(j)}]) \right)^2 \right], \\
&\leq \mathbb{E} \left[\sum_{j=1}^J 1^2 \cdot \sum_{j=1}^J (X^{(j)} - \mathbb{E} [X^{(j)}])^2 \right], \\
&= J \sum_{j=1}^J \mathbb{E} \left[(X^{(j)} - \mathbb{E} [X^{(j)}])^2 \right], \\
(118) \quad &= J \sum_{j=1}^J \mathbb{V} [X^{(j)}].
\end{aligned}$$

Equality holds for independent random variables.

APPENDIX B. PROOF OF REMARK 9

Proof. First, we assumed that $N_e = d_y = 1$. Next, from (95), the numerator in the logarithm in (98) is given by the following:

$$(119) \quad \begin{aligned} & \int_{\mathbb{R}} \log \left(\frac{1}{\sqrt{2\pi\sigma_\varepsilon^2}} \exp \left(-\frac{\varepsilon^2}{2\sigma_\varepsilon^2} \right) \right) \frac{1}{\sqrt{2\pi\sigma_\varepsilon^2}} \exp \left(-\frac{\varepsilon^2}{2\sigma_\varepsilon^2} \right) d\varepsilon \\ &= -\frac{1}{2} \log(2\pi\sigma_\varepsilon^2) - \frac{1}{\sqrt{2\pi\sigma_\varepsilon^2}} \frac{1}{2\sigma_\varepsilon^2} \int_{\mathbb{R}} \varepsilon^2 \exp \left(-\frac{\varepsilon^2}{2\sigma_\varepsilon^2} \right) d\varepsilon. \end{aligned}$$

We define $s := 1/(2\sigma_\varepsilon^2)$ and solve the integral in (119) by taking the derivative with respect to s :

$$(120) \quad \begin{aligned} \int_{\mathbb{R}} \varepsilon^2 e^{-s\varepsilon^2} d\varepsilon &= -\int_{\mathbb{R}} \frac{\partial}{\partial s} e^{-s\varepsilon^2} d\varepsilon = -\frac{\partial}{\partial s} \int_{\mathbb{R}} e^{-s\varepsilon^2} d\varepsilon = -\sqrt{\pi} \frac{\partial}{\partial s} s^{-\frac{1}{2}} \\ &= \sqrt{\frac{\pi}{s}} \frac{1}{2s} = \sqrt{2\pi\sigma_\varepsilon^2} \sigma_\varepsilon^2. \end{aligned}$$

Inserting this into (119) changes the numerator in (98) to $-(\log(2\pi\sigma_\varepsilon^2) + 1)/2$. The case for $\varepsilon_i \in \mathbb{R}^{d_y}$, where $1 \leq i \leq N_e$, follows trivially under the hypothesis. \square

APPENDIX C. VERIFICATION OF ASSUMPTION 1 FOR THE EIG

To verify Assumption 1 for the nested integrand in the EIG (98), we introduce the notation

$$(121) \quad \tilde{\mathbf{G}}(\cdot) := \mathbf{G}(F_\theta^{-1}(\cdot), \boldsymbol{\xi}),$$

where F_θ^{-1} is the inverse CDF of the parameters of interest $\boldsymbol{\theta}$ and the dependence on the design $\boldsymbol{\xi}$ has been omitted and state the following:

Assumption 7 (Conditions on the experiment model). *Let $\tilde{\mathbf{G}} : [0, 1]^{d_2} \rightarrow \mathbb{R}^{d_1-d_2}$ be such that*

$$(122) \quad \left\| \left(\prod_{j \in u} \frac{\partial^u}{\partial z_j} \right) \tilde{\mathbf{G}}(\mathbf{z}) \right\|_2 \leq L < \infty$$

for all $\mathbf{z} \in [0, 1]^{d_2}$, and all $u \subseteq \{1, \dots, d_2\}$. Moreover, let $\tilde{\mathbf{G}}$ be Lipschitz continuous, that is,

$$(123) \quad \left\| \tilde{\mathbf{G}}(\mathbf{z}) - \tilde{\mathbf{G}}(\mathbf{z}') \right\|_2 \leq L \|\mathbf{z} - \mathbf{z}'\|_2,$$

for $\mathbf{z}, \mathbf{z}' \in [0, 1]^{d_2}$, where $0 < L < \infty$ is a constant.

Lipschitz continuity (123) of the function $\tilde{\mathbf{G}}$ is a consequence of the differentiability condition (122), and was stated for exposition.

Lemma 1 (Verification of Assumption 1 for the EIG). *Let $f \equiv \log$ and $g : [0, 1]^{d_1} \times [0, 1]^{d_2} \rightarrow \mathbb{R}$, where*

$$(124) \quad g(\mathbf{y}, \mathbf{x}) = \frac{1}{\det(2\pi\boldsymbol{\Sigma}_\varepsilon)^{\frac{1}{2}}} e^{-\frac{1}{2} \left\| \tilde{\mathbf{G}}(\mathbf{y}_1) + \boldsymbol{\Sigma}_\varepsilon^{\frac{1}{2}} \Phi^{-1}(\mathbf{y}_2) - \tilde{\mathbf{G}}(\mathbf{x}) \right\|_{\boldsymbol{\Sigma}_\varepsilon^{-1}}^2},$$

where $d_1 > d_2$, $\mathbf{y} = (\mathbf{y}_1, \mathbf{y}_2) \in [0, 1]^{d_1}$, $\mathbf{y}_1, \mathbf{x} \in [0, 1]^{d_2}$, $\mathbf{y}_2 \in [0, 1]^{d_1-d_2}$, and $\tilde{\mathbf{G}} : [0, 1]^{d_2} \rightarrow \mathbb{R}^{d_1-d_2}$ satisfies Assumption 7. Moreover, $\boldsymbol{\Sigma}_\varepsilon \in \mathbb{R}^{(d_1-d_2) \times (d_1-d_2)}$ is a positive definite matrix and Φ^{-1} is the inverse CDF of the standard normal in dimension $d_1 - d_2$ and define:

$$(125) \quad \tilde{f} := f \left(\int_{[0, 1]^{d_2}} g(\mathbf{y}, \mathbf{x}) d\mathbf{x} \right).$$

For the conditions stated in Assumption 1, it holds for the nested integrand \tilde{f} that

$$(126) \quad \left| \left(\prod_{j \in u} \frac{\partial^u}{\partial y_j} \right) \tilde{f}(\mathbf{y}) \right| \leq b \prod_{i=1}^{d_1} \min(y_i, 1 - y_i)^{-A_i - \mathbb{1}_{\{i \in u\}}},$$

for all $\mathbf{y} \in (0, 1)^{d_1}$ and all $u \subseteq \{1, \dots, d_1\}$, $0 < b < \infty$, $A_i > 0$, $1 \leq i \leq d_1$, and $\max_i A_i < 1/2$.

Proof. For illustration, we assumed that $d_1 = 2$, $d_2 = 1$, and $\Sigma_\epsilon = 1$, which results in

$$(127) \quad g(\mathbf{y}, x) = \frac{1}{\sqrt{2\pi}} e^{-\frac{1}{2}(\tilde{G}(y_1) + \Phi^{-1}(y_2) - \tilde{G}(x))^2}.$$

Moreover, we require that

$$(128) \quad \left| \frac{\partial^2}{\partial y_1 \partial y_2} \tilde{f}(y_1, y_2) \right| \leq b \min(y_1, 1 - y_1)^{-A_1 - 1} \min(y_2, 1 - y_2)^{-A_2 - 1},$$

$$(129) \quad \left| \frac{\partial}{\partial y_1} \tilde{f}(y_1, y_2) \right| \leq b \min(y_1, 1 - y_1)^{-A_1 - 1} \min(y_2, 1 - y_2)^{-A_2},$$

$$(130) \quad \left| \frac{\partial}{\partial y_2} \tilde{f}(y_1, y_2) \right| \leq b \min(y_1, 1 - y_1)^{-A_1} \min(y_2, 1 - y_2)^{-A_2 - 1},$$

$$(131) \quad \left| \tilde{f}(y_1, y_2) \right| \leq b \min(y_1, 1 - y_1)^{-A_1} \min(y_2, 1 - y_2)^{-A_2},$$

where

$$(132) \quad \tilde{f}(y_1, y_2) \equiv \log \left(\frac{1}{\sqrt{2\pi}} \int_{[0,1]} e^{-\frac{1}{2}(\tilde{G}(y_1) + \Phi^{-1}(y_2) - \tilde{G}(x))^2} dx \right).$$

The Condition (129) yields the following:

$$(133) \quad \left| \frac{\partial}{\partial y_1} \tilde{f}(y_1, y_2) \right| = \left| \frac{\int_{[0,1]} \left(\tilde{G}(y_1) + \Phi^{-1}(y_2) - \tilde{G}(x) \right) \frac{d}{dy_1} \tilde{G}(y_1) e^{-\frac{1}{2}(\tilde{G}(y_1) + \Phi^{-1}(y_2) - \tilde{G}(x))^2} dx}{\int_{[0,1]} e^{-\frac{1}{2}(\tilde{G}(y_1) + \Phi^{-1}(y_2) - \tilde{G}(x))^2} dx} \right|,$$

$$\leq \max_{x \in [0,1]} \left\{ \left| \left(\tilde{G}(y_1) + \Phi^{-1}(y_2) - \tilde{G}(x) \right) \frac{d}{dy_1} \tilde{G}(y_1) \right| \right\},$$

$$\leq L (L + |\Phi^{-1}(y_2)|)$$

by Assumption 7. For the case in which $y_2 \rightarrow 0^+$, the following approximation is employed [43, 42, 65]:

$$(134) \quad \Phi^{-1}(y_2) = -\sqrt{-2 \log(y_2)} + o(1),$$

for which it holds that

$$(135) \quad |\Phi^{-1}(y_2)| \leq \sqrt{-2 \log(y_2)} + P,$$

for any $P > 0$ and all $y_2 \leq y_{2,0}$ for some $y_{2,0} \in (0, 1)$ as $y_2 \rightarrow 0^+$. Next, we apply the inequality

$$(136) \quad \begin{aligned} \sqrt{2} \sqrt{\log(y_2^{-1})} &\leq A_2 \log(y_2^{-1}), \\ &\leq y_2^{-A_2}, \end{aligned}$$

for any $A_2 > 0$ as $y_2 \rightarrow 0^+$ to obtain

$$(137) \quad \begin{aligned} \left| \frac{\partial}{\partial y_1} \tilde{f}(y_1, y_2) \right| &\leq L (L + |\Phi^{-1}(y_2)|), \\ &\leq L (L + y_2^{-A_2} + P). \end{aligned}$$

The case in which $y_2 \rightarrow 1^-$ follows by a similar derivation, employing the following approximation [43, 42, 65]:

$$(138) \quad \Phi^{-1}(y_2) = -\sqrt{-2 \log(1 - y_2)} + o(1).$$

Finally,

$$(139) \quad \left| \frac{\partial}{\partial y_1} \tilde{f}(y_1, y_2) \right| \leq b_1 \min(y_1, 1 - y_1)^{-A_1 - 1} \min(y_2, 1 - y_2)^{-A_2}$$

for $0 < b_1 < \infty$ and any $A_1, A_2 > 0$. The Condition (130) yields the following:

$$\begin{aligned}
\left| \frac{\partial}{\partial y_2} \tilde{f}(y_1, y_2) \right| &= \left| \frac{\int_{[0,1]} \left(\tilde{G}(y_1) + \Phi^{-1}(y_2) - \tilde{G}(x) \right) \frac{d}{dy_2} \Phi^{-1}(y_2) e^{-\frac{1}{2}(\tilde{G}(y_1) + \Phi^{-1}(y_2) - \tilde{G}(x))^2} dx}{\int_{[0,1]} e^{-\frac{1}{2}(\tilde{G}(y_1) + \Phi^{-1}(y_2) - \tilde{G}(x))^2} dx} \right|, \\
(140) \quad &\leq \max_{x \in [0,1]} \left\{ \left| \left(\tilde{G}(y_1) + \Phi^{-1}(y_2) - \tilde{G}(x) \right) \frac{d}{dy_2} \Phi^{-1}(y_2) \right| \right\}, \\
&\leq \left| \frac{d}{dy_2} \Phi^{-1}(y_2) \right| (L + |\Phi^{-1}(y_2)|).
\end{aligned}$$

It follows that

$$\begin{aligned}
\frac{d}{dy_2} \Phi^{-1}(y_2) &= (\Phi'(\Phi^{-1}(y_2)))^{-1}, \\
(141) \quad &= \sqrt{2\pi} e^{\frac{1}{2}(\Phi^{-1}(y_2))^2},
\end{aligned}$$

yielding

$$\begin{aligned}
\frac{d}{dy_2} \Phi^{-1}(y_2) &= \sqrt{2\pi} e^{\frac{1}{2}(\Phi^{-1}(y_2))^2}, \\
&= \sqrt{2\pi} e^{\frac{1}{2}(-\sqrt{-2\log(y_2)} + o(1))^2}, \\
&= \sqrt{2\pi} e^{(\log(y_2^{-1}) + o(\sqrt{\log(y_2^{-1})}) + o(1))}, \\
&\leq \sqrt{2\pi} e^{(\log(y_2^{-1}) + P\sqrt{\log(y_2^{-1})} + P)}, \\
&\leq \sqrt{2\pi} e^{(\log(y_2^{-1}) + B_2 \log(y_2^{-1}) + P)}, \\
(142) \quad &= \sqrt{2\pi} e^P y_2^{-B_2-1}.
\end{aligned}$$

for any $P, B_2 > 0$ and all $y_2 \leq y_{2,0}$ for some $y_{2,0} \in (0, 1)$ as $y_2 \rightarrow 0^+$. Thus, it follows that

$$\begin{aligned}
|\Phi^{-1}(y_2)| \left| \frac{d}{dy_2} \Phi^{-1}(y_2) \right| &\leq \left(\sqrt{-2\log(y_2)} + P \right) \sqrt{2\pi} e^P y_2^{-B_2-1}, \\
(143) \quad &\leq \left(y_2^{-C_2} + P \right) \sqrt{2\pi} e^P y_2^{-B_2-1},
\end{aligned}$$

for any $C_2 > 0$ as $y_2 \rightarrow 0^+$. The case in which $y_2 \rightarrow 1^-$ again follows from the application of the Approximation in (138). Finally,

$$(144) \quad \left| \frac{\partial}{\partial y_2} \tilde{f}(y_1, y_2) \right| \leq b_2 \min(y_1, 1 - y_1)^{-A_1} \min(y_2, 1 - y_2)^{-A_2-1}$$

for $0 < b_2 < \infty$, any $A_1 > 0$, and any $A_2 := B_2 + C_2 > 0$. Condition (128) follows by a similar derivation for $0 < b_3$ and any $A_1, A_2 > 0$. For Condition (131), Assumption 123 was used to obtain the following:

$$\begin{aligned}
& \left| \log \left(\int_{[0,1]} e^{-\frac{1}{2}(\tilde{G}(y_1) + \Phi^{-1}(y_2) - \tilde{G}(x))^2} dx \right) \right| \\
&= \left| \log \left(\int_{[0,1]} e^{-\frac{1}{2}((\tilde{G}(y_1) - \tilde{G}(x))^2 + 2(\tilde{G}(y_1) - \tilde{G}(x))\Phi^{-1}(y_2) + (\Phi^{-1}(y_2))^2)} dx \right) \right| \\
&\leq \left| \log \left(\int_{[0,1]} e^{-\frac{1}{2}((\tilde{G}(y_1) - \tilde{G}(x))^2 + 2|\tilde{G}(y_1) - \tilde{G}(x)| |\Phi^{-1}(y_2)| + (\Phi^{-1}(y_2))^2)} dx \right) \right| \\
&\leq \left| \log \left(\int_{[0,1]} e^{-\frac{1}{2}(L^2(y_1-x)^2 + 2L|y_1-x| |\Phi^{-1}(y_2)| + (\Phi^{-1}(y_2))^2)} dx \right) \right| \\
&\leq \left| \log \left(e^{-\frac{1}{2}(L^2 + 2L|\Phi^{-1}(y_2)| + (\Phi^{-1}(y_2))^2)} \right) \right| \\
(145) \quad &= \left| \frac{1}{2}L^2 + L|\Phi^{-1}(y_2)| + \frac{1}{2}(\Phi^{-1}(y_2))^2 \right|.
\end{aligned}$$

The approximation (134) as $y_2 \rightarrow 0^+$ was used to obtain:

$$\begin{aligned}
\left| \frac{1}{2}L^2 + L|\Phi^{-1}(y_2)| + (\Phi^{-1}(y_2))^2 \right| &= \left| \frac{1}{2}L^2 + L \left| -\sqrt{-2\log(y_2)} + o(1) \right| + \left(-\sqrt{-2\log(y_2)} + o(1) \right)^2 \right|, \\
&\leq \left| \frac{1}{2}L^2 + L\sqrt{2}\sqrt{\log(y_2^{-1})} + LP + \log(y_2^{-1}) + P\sqrt{2}\sqrt{\log(y_2^{-1})} + \frac{1}{2}P \right|, \\
&= \left| \frac{1}{2}L^2 + (L+P)\sqrt{2}\sqrt{\log(y_2^{-1})} + LP + \log(y_2^{-1}) + \frac{1}{2}P \right|, \\
(146) \quad &\leq \left| \frac{1}{2}L^2 + (L+P)\sqrt{2}y_2^{-C_2} + LP + y_2^{-B_2} + \frac{1}{2}P \right|
\end{aligned}$$

for any $B_2, C_2 > 0$. The case in which $y_2 \rightarrow 1^-$ follows from the application of the Approximation in (138), providing

$$(147) \quad \left| \tilde{f}(y_1, y_2) \right| \leq b_4 \min(y_1, 1 - y_1)^{-A_1} \min(y_2, 1 - y_2)^{-A_2}$$

for $0 < b_4 < \infty$, any A_1 , and any $A_2 := \max\{B_2, C_2\} > 0$. Setting $b := \max_{i \in \{1, \dots, 4\}} b_i$ demonstrates the Conditions (128) to (131). Moreover, the general case in higher dimensions can be demonstrated using the Faà di Bruno formula. \square

APPENDIX D. VERIFICATION OF CONDITION (42) FOR THE EIG

To verify Condition (40), we assume the same setting as in Lemma 1 and set

$$\begin{aligned}
I &= \int_{[0,1]^2} \log \left(\frac{1}{\sqrt{2\pi}} \int_{[0,1]} e^{-\frac{1}{2}(\tilde{G}(y_1) + \Phi^{-1}(y_2) - \tilde{G}(x))^2} dx \right) dy_2 dy_1, \\
&= \int_{[0,1]} \int_{\mathbb{R}} \log \left(\frac{1}{\sqrt{2\pi}} \int_{[0,1]} e^{-\frac{1}{2}(\tilde{G}(y_1) + \varepsilon - \tilde{G}(x))^2} dx \right) \frac{1}{\sqrt{2\pi}} e^{-\frac{1}{2}\varepsilon^2} d\varepsilon dy_1, \\
&= \int_{[0,1]} \int_{-c(TOL)}^{c(TOL)} \log \left(\frac{1}{\sqrt{2\pi}} \int_{[0,1]} e^{-\frac{1}{2}(\tilde{G}(y_1) + \varepsilon - \tilde{G}(x))^2} dx \right) \frac{1}{\sqrt{2\pi}} e^{-\frac{1}{2}\varepsilon^2} d\varepsilon dy_1, \\
&\quad + \int_{[0,1]} \int_{-\infty}^{-c(TOL)} \log \left(\frac{1}{\sqrt{2\pi}} \int_{[0,1]} e^{-\frac{1}{2}(\tilde{G}(y_1) + \varepsilon - \tilde{G}(x))^2} dx \right) \frac{1}{\sqrt{2\pi}} e^{-\frac{1}{2}\varepsilon^2} d\varepsilon dy_1, \\
&\quad + \int_{[0,1]} \int_{c(TOL)}^{\infty} \log \left(\frac{1}{\sqrt{2\pi}} \int_{[0,1]} e^{-\frac{1}{2}(\tilde{G}(y_1) + \varepsilon - \tilde{G}(x))^2} dx \right) \frac{1}{\sqrt{2\pi}} e^{-\frac{1}{2}\varepsilon^2} d\varepsilon dy_1, \\
&= I^{\text{tr}} + \int_{[0,1]} \int_{-\infty}^{-c(TOL)} \log \left(\frac{1}{\sqrt{2\pi}} \int_{[0,1]} e^{-\frac{1}{2}(\tilde{G}(y_1) + \varepsilon - \tilde{G}(x))^2} dx \right) \frac{1}{\sqrt{2\pi}} e^{-\frac{1}{2}\varepsilon^2} d\varepsilon dy_1, \\
&\quad + \int_{[0,1]} \int_{c(TOL)}^{\infty} \log \left(\frac{1}{\sqrt{2\pi}} \int_{[0,1]} e^{-\frac{1}{2}(\tilde{G}(y_1) + \varepsilon - \tilde{G}(x))^2} dx \right) \frac{1}{\sqrt{2\pi}} e^{-\frac{1}{2}\varepsilon^2} d\varepsilon dy_1,
\end{aligned} \tag{148}$$

where

$$c(TOL) := (2(1+p))^{\frac{1}{2}} \log(TOL^{-1})^{\frac{1}{2}}, \tag{149}$$

for any $p > 0$, signifies a region of truncation for a tolerance $TOL > 0$ and

$$\begin{aligned}
I^{\text{tr}} &= \int_{[0,1]} \int_{-c(TOL)}^{c(TOL)} \log \left(\frac{1}{\sqrt{2\pi}} \int_{[0,1]} e^{-\frac{1}{2}(\tilde{G}(y_1) + \varepsilon - \tilde{G}(x))^2} dx \right) \frac{1}{\sqrt{2\pi}} e^{-\frac{1}{2}\varepsilon^2} d\varepsilon dy_1, \\
&= \int_{[0,1]^2} \log \left(\frac{1}{\sqrt{2\pi}} \int_{[0,1]} e^{-\frac{1}{2}(\tilde{G}(y_1) + F_{c(TOL)}^{-1}(y_2) - \tilde{G}(x))^2} dx \right) dy_2 dy_1,
\end{aligned} \tag{150}$$

where

$$F_{c(TOL)}^{-1}(y_2) := \Phi^{-1} \left((2\Phi(c(TOL)) - 1)y_2 + (1 - \Phi(c(TOL))) \right) \tag{151}$$

is the inverse CDF of the standard normal distribution truncated to the interval $[-c(TOL), c(TOL)]$.

Lemma 2 (Verification of Condition (40) for the EIG). *Given the assumptions of Lemma 1 for $F_{c(TOL)}^{-1}(y_2)$ instead of $\Phi^{-1}(y_2)$, for a fixed and sufficiently small value of $c(TOL)$ as in (149), where $TOL > 0$, the Condition (40) for a constant $k < \infty$ is verified, where*

$$\sup_{\mathbf{y} \in [0,1]^2} \left| \frac{V_{\text{HK}}(g(\mathbf{y}, \cdot))}{\tilde{g}(\mathbf{y})} \right| < \tilde{L}c(TOL) < \infty, \tag{152}$$

where $\tilde{L} > 0$.

Proof. The Hardy–Krause variation is as follows:

$$\begin{aligned}
V_{\text{HK}}(g(\mathbf{y}, \cdot)) &= \int_{[0,1]} \left| \frac{\partial}{\partial x} \frac{1}{\sqrt{2\pi}Z} e^{-\frac{1}{2}(\tilde{G}(y_1) + F_{c(TOL)}^{-1}(y_2) - \tilde{G}(x))^2} \right| dx, \\
&= \frac{1}{\sqrt{2\pi}Z} \int_{[0,1]} \left| \left(\tilde{G}(y_1) + F_{c(TOL)}^{-1}(y_2) - \tilde{G}(x) \right) \frac{d}{dx} \tilde{G}(x) e^{-\frac{1}{2}(\tilde{G}(y_1) + F_{c(TOL)}^{-1}(y_2) - \tilde{G}(x))^2} \right| dx, \\
&= \frac{1}{\sqrt{2\pi}Z} \int_{[0,1]} \left| \frac{d}{dx} \tilde{G}(x) \right| \left| \left(\tilde{G}(y_1) + F_{c(TOL)}^{-1}(y_2) - \tilde{G}(x) \right) e^{-\frac{1}{2}(\tilde{G}(y_1) + F_{c(TOL)}^{-1}(y_2) - \tilde{G}(x))^2} \right| dx, \\
&\leq \frac{1}{\sqrt{2\pi}Z} \int_{[0,1]} \left| \frac{d}{dx} \tilde{G}(x) \right| dx, \\
(153) \quad &\leq \frac{L}{\sqrt{2\pi}Z},
\end{aligned}$$

where Z denotes the normalization constant of the standard normal distribution truncated to the interval $[-c(TOL), c(TOL)]$. For Condition (40),

$$\begin{aligned}
&\sup_{\mathbf{y} \in [0,1]^2} \left| \frac{\frac{1}{\sqrt{2\pi}} \int_{[0,1]} \left| \left(\tilde{G}(y_1) + F_{c(TOL)}^{-1}(y_2) - \tilde{G}(x) \right) \frac{d}{dx} \tilde{G}(x) e^{-\frac{1}{2}(\tilde{G}(y_1) + F_{c(TOL)}^{-1}(y_2) - \tilde{G}(x))^2} \right| dx}{\frac{1}{\sqrt{2\pi}} \int_{[0,1]} e^{-\frac{1}{2}(\tilde{G}(y_1) + F_{c(TOL)}^{-1}(y_2) - \tilde{G}(x))^2} dx} \right| \\
&\leq \sup_{\mathbf{y} \in [0,1]^2} \left| \max_{x \in [0,1]} \left\{ \left(\tilde{G}(y_1) + F_{c(TOL)}^{-1}(y_2) - \tilde{G}(x) \right) \frac{d}{dx} \tilde{G}(x) \right\} \right|, \\
(154) \quad &\leq L \left(L + \sup_{\mathbf{y} \in [0,1]^2} \left| F_{c(TOL)}^{-1}(y_2) \right| \right).
\end{aligned}$$

The CDF $\Phi(\cdot)$ of the standard normal and its inverse are monotonic; hence, the supremum of $|F_{c(TOL)}^{-1}(y_2)|$ is attained at $y_2 \in \{0, 1\}$, yielding

$$(155) \quad \sup_{y_2 \in [0,1]} |F_{c(TOL)}^{-1}(y_2)| = c(TOL),$$

with $c(TOL)$ as in (149). It follows that

$$\begin{aligned}
&\sup_{\mathbf{y} \in [0,1]^2} \left| \frac{\frac{1}{\sqrt{2\pi}} \int_{[0,1]} \left| \left(\tilde{G}(y_1) + F_{c(TOL)}^{-1}(y_2) - \tilde{G}(x) \right) \frac{d}{dx} \tilde{G}(x) e^{-\frac{1}{2}(\tilde{G}(y_1) + F_{c(TOL)}^{-1}(y_2) - \tilde{G}(x))^2} \right| dx}{\frac{1}{\sqrt{2\pi}} \int_{[0,1]} e^{-\frac{1}{2}(\tilde{G}(y_1) + F_{c(TOL)}^{-1}(y_2) - \tilde{G}(x))^2} dx} \right| \\
(156) \quad &\leq \tilde{L}c(TOL)
\end{aligned}$$

for TOL sufficiently small, where $\tilde{L} > 0$ depends on the Lipschitz constant L of G . The general case in higher dimensions can also be demonstrated using the Faà di Bruno formula. \square

The constant $k = \tilde{L}c(TOL)$ in Condition (40) thus displays only weak dependence on the error tolerance (TOL). For observation noise from a truncated Gaussian distribution, Proposition 2 is not required to bound the rQMC error; the Koksma–Hlawka inequality (8) is sufficient.

APPENDIX E. BOUND ON THE TRUNCATION ERROR OF THE NESTED INTEGRAL IN THE EIG

Lemma 3 (Bound on the truncation error of the nested integral in the EIG). *Given the assumptions of Lemma 2, the truncation error is bounded as*

$$(157) \quad |I - I^{\text{tr}}| = o(TOL),$$

where I as in (148) and I^{tr} as in (150), as $TOL \rightarrow 0$.

Proof. By the triangle inequality,

$$\begin{aligned}
|I - I^{\text{tr}}| &= \left| \int_{[0,1]} \int_{-\infty}^{-c(TOL)} \log \left(\frac{1}{\sqrt{2\pi}} \int_{[0,1]} e^{-\frac{1}{2}(\tilde{G}(y_1)+\varepsilon-\tilde{G}(x))^2} dx \right) \frac{1}{\sqrt{2\pi}} e^{-\frac{1}{2}\varepsilon^2} d\varepsilon dy_1 \right. \\
&\quad \left. + \int_{[0,1]} \int_{c(TOL)}^{\infty} \log \left(\frac{1}{\sqrt{2\pi}} \int_{[0,1]} e^{-\frac{1}{2}(\tilde{G}(y_1)+\varepsilon-\tilde{G}(x))^2} dx \right) \frac{1}{\sqrt{2\pi}} e^{-\frac{1}{2}\varepsilon^2} d\varepsilon dy_1 \right|, \\
(158) \quad &\leq \left| \int_{[0,1]} \int_{-\infty}^{-c(TOL)} \log \left(\frac{1}{\sqrt{2\pi}} \int_{[0,1]} e^{-\frac{1}{2}(\tilde{G}(y_1)+\varepsilon-\tilde{G}(x))^2} dx \right) \frac{1}{\sqrt{2\pi}} e^{-\frac{1}{2}\varepsilon^2} d\varepsilon dy_1 \right| \\
&\quad + \left| \int_{[0,1]} \int_{c(TOL)}^{\infty} \log \left(\frac{1}{\sqrt{2\pi}} \int_{[0,1]} e^{-\frac{1}{2}(\tilde{G}(y_1)+\varepsilon-\tilde{G}(x))^2} dx \right) \frac{1}{\sqrt{2\pi}} e^{-\frac{1}{2}\varepsilon^2} d\varepsilon dy_1 \right|.
\end{aligned}$$

By Jensen's inequality it follows that

$$\begin{aligned}
\frac{1}{2} \left(\tilde{G}(y_1) + \varepsilon - \tilde{G}(x) \right)^2 &= 2 \left(\frac{\tilde{G}(y_1) - \tilde{G}(x)}{2} + \frac{\varepsilon}{2} \right)^2, \\
&\leq 2 \left(\frac{(\tilde{G}(y_1) - \tilde{G}(x))^2}{2} + \frac{\varepsilon^2}{2} \right), \\
(159) \quad &= (\tilde{G}(y_1) - \tilde{G}(x))^2 + \varepsilon^2,
\end{aligned}$$

and thus for the last term in (158) that

$$\begin{aligned}
&\left| \int_{[0,1]} \int_{c(TOL)}^{\infty} \log \left(\frac{1}{\sqrt{2\pi}} \int_{[0,1]} e^{-\frac{1}{2}(\tilde{G}(y_1)+\varepsilon-\tilde{G}(x))^2} dx \right) \frac{1}{\sqrt{2\pi}} e^{-\frac{1}{2}\varepsilon^2} d\varepsilon dy_1 \right| \\
&\leq \int_{[0,1]} \int_{c(TOL)}^{\infty} \left| \log \left(\frac{1}{\sqrt{2\pi}} \int_{[0,1]} e^{-\frac{1}{2}(\tilde{G}(y_1)+\varepsilon-\tilde{G}(x))^2} dx \right) \right| \frac{1}{\sqrt{2\pi}} e^{-\frac{1}{2}\varepsilon^2} d\varepsilon dy_1, \\
(160) \quad &\leq \int_{[0,1]} \int_{c(TOL)}^{\infty} \left| \log \left(\frac{1}{\sqrt{2\pi}} \int_{[0,1]} e^{-(\tilde{G}(y_1)-\tilde{G}(x))^2-\varepsilon^2} dx \right) \right| \frac{1}{\sqrt{2\pi}} e^{-\frac{1}{2}\varepsilon^2} d\varepsilon dy_1.
\end{aligned}$$

Next, from Assumption 7 it follows that

$$\begin{aligned}
&\int_{[0,1]} \int_{c(TOL)}^{\infty} \left| \log \left(\frac{1}{\sqrt{2\pi}} \int_{[0,1]} e^{-(\tilde{G}(y_1)-\tilde{G}(x))^2-\varepsilon^2} dx \right) \right| \frac{1}{\sqrt{2\pi}} e^{-\frac{1}{2}\varepsilon^2} d\varepsilon dy_1, \\
&\leq \int_{[0,1]} \int_{c(TOL)}^{\infty} \left| \log \left(\frac{1}{\sqrt{2\pi}} \int_{[0,1]} e^{-L^2(y_1-x)^2-\varepsilon^2} dx \right) \right| \frac{1}{\sqrt{2\pi}} e^{-\frac{1}{2}\varepsilon^2} d\varepsilon dy_1, \\
&< \int_{c(TOL)}^{\infty} \left| \log \left(\frac{1}{\sqrt{2\pi}} e^{-L^2-\varepsilon^2} \right) \right| \frac{1}{\sqrt{2\pi}} e^{-\frac{1}{2}\varepsilon^2} d\varepsilon, \\
&= \int_{c(TOL)}^{\infty} |T - \varepsilon^2| \frac{1}{\sqrt{2\pi}} e^{-\frac{1}{2}\varepsilon^2} d\varepsilon, \\
(161) \quad &\leq \int_{c(TOL)}^{\infty} |T| \frac{1}{\sqrt{2\pi}} e^{-\frac{1}{2}\varepsilon^2} d\varepsilon + \int_{c(TOL)}^{\infty} \varepsilon^2 \frac{1}{\sqrt{2\pi}} e^{-\frac{1}{2}\varepsilon^2} d\varepsilon,
\end{aligned}$$

where $T := -L^2 - \log(\sqrt{2\pi})$. The first term in (161) is bounded via integration by parts,

$$\begin{aligned}
\int_{c(TOL)}^{\infty} |T| \frac{1}{\sqrt{2\pi}} e^{-\frac{1}{2}\varepsilon^2} d\varepsilon &= |T| \frac{1}{\sqrt{2\pi}} \int_{c(TOL)}^{\infty} \frac{1}{\varepsilon} \cdot \varepsilon e^{-\frac{1}{2}\varepsilon^2} d\varepsilon, \\
&= |T| \frac{1}{\sqrt{2\pi}} \left(\left[-\frac{1}{\varepsilon} e^{-\frac{1}{2}\varepsilon^2} \right]_{c(TOL)}^{\infty} - \int_{c(TOL)}^{\infty} \frac{1}{\varepsilon^2} e^{-\frac{1}{2}\varepsilon^2} d\varepsilon \right), \\
&= |T| \frac{1}{\sqrt{2\pi}} \left(\frac{1}{c(TOL)} e^{-\frac{1}{2}(c(TOL))^2} - \int_{c(TOL)}^{\infty} \frac{1}{\varepsilon^2} e^{-\frac{1}{2}\varepsilon^2} d\varepsilon \right), \\
(162) \quad &< |T| \frac{1}{\sqrt{2\pi}} \frac{1}{c(TOL)} e^{-\frac{1}{2}(c(TOL))^2},
\end{aligned}$$

where the last term in the second to last line is strictly positive. Substituting (149) into (162), we find that

$$\begin{aligned}
\int_{c(TOL)}^{\infty} |T| \frac{1}{\sqrt{2\pi}} e^{-\frac{1}{2}\varepsilon^2} d\varepsilon &< |T| \frac{1}{\sqrt{2\pi}} (2(1+p))^{-\frac{1}{2}} \log(TOL^{-1})^{-\frac{1}{2}} TOL^{1+p}, \\
(163) \quad &= o(TOL)
\end{aligned}$$

as $TOL \rightarrow 0$. The second term in (161) is bounded via integration by parts as

$$\begin{aligned}
\int_{c(TOL)}^{\infty} \varepsilon^2 \frac{1}{\sqrt{2\pi}} e^{-\frac{1}{2}\varepsilon^2} d\varepsilon &= \frac{1}{\sqrt{2\pi}} \int_{c(TOL)}^{\infty} \varepsilon \cdot \varepsilon e^{-\frac{1}{2}\varepsilon^2} d\varepsilon, \\
&= \frac{1}{\sqrt{2\pi}} \left[-\varepsilon e^{-\frac{1}{2}\varepsilon^2} \right]_{c(TOL)}^{\infty} + \frac{1}{\sqrt{2\pi}} \int_{c(TOL)}^{\infty} e^{-\frac{1}{2}\varepsilon^2} d\varepsilon, \\
&= \frac{1}{\sqrt{2\pi}} c(TOL) e^{-\frac{1}{2}(c(TOL))^2} + \frac{1}{\sqrt{2\pi}} \int_{c(TOL)}^{\infty} e^{-\frac{1}{2}\varepsilon^2} d\varepsilon, \\
&< \frac{1}{\sqrt{2\pi}} c(TOL) e^{-\frac{1}{2}(c(TOL))^2} + \frac{1}{\sqrt{2\pi}} \frac{1}{c(TOL)} e^{-\frac{1}{2}(c(TOL))^2}, \\
&< \frac{1}{\sqrt{2\pi}} (2(1+p))^{\frac{1}{2}} \log(TOL^{-1})^{\frac{1}{2}} TOL^{1+p} + \frac{1}{\sqrt{2\pi}} (2(1+p))^{-\frac{1}{2}} \log(TOL^{-1})^{-\frac{1}{2}} TOL^{1+p}, \\
(164) \quad &= o(TOL)
\end{aligned}$$

as $TOL \rightarrow 0$ by a similar derivation as in (162). The bound on the first term in (158) follows analogously. Finally, it holds that

$$\begin{aligned}
|I - I^{\text{tr}}| &< \frac{2}{\sqrt{2\pi}} \left((2(1+p))^{\frac{1}{2}} \log(TOL^{-1})^{\frac{1}{2}} + (1+|T|)(2(1+p))^{-\frac{1}{2}} \log(TOL^{-1})^{-\frac{1}{2}} \right) TOL^{1+p}, \\
(165) \quad &= o(TOL).
\end{aligned}$$

□

Remark 11 (Extension to more general noise distributions). *This derivation can be generalized to other noise distributions, however, distributions with fatter tails than a Gaussian would result in a different truncation parameter $c(TOL)$.*

Remark 12 (Extensions to general dimensions). *The case for dimension $d > 1$ follows immediately for a diagonal covariance matrix $\Sigma_{\varepsilon} = \mathbf{I}_{d \times d}$, yielding only weak dependence of the truncation error on the integrand dimension.*

APPENDIX F. TOTAL ERROR OF THE EIG ESTIMATION VIA THE rDLQMC ESTIMATOR

Corollary 1 (Total error of the EIG estimation via the rDLQMC estimator). *Under the assumptions stated in Proposition 3, Proposition 4, Lemma 2, and Lemma 3, it holds that*

$$(166) \quad |I - I^{\text{tr}}| = o(\text{TOL}),$$

(167)

$$(168) \quad \begin{aligned} |E[I_{\text{rDLQ}}^{\text{tr}}] - I^{\text{tr}}| &\leq C_{\text{disc}} h^\eta + \frac{\mathbb{E}[|\bar{g}|^2 |f''(\bar{g})|] \tilde{L}^2(c(\text{TOL}))^2 C_{\epsilon, d_2}^2}{2M^{2-2\epsilon}} + \frac{\mathbb{E}[|\bar{g}|^3 |f'''(K(\text{TOL})\bar{g})|] \tilde{L}^3(c(\text{TOL}))^3 C_{\epsilon, d_2}^3}{6M^{3-3\epsilon}}, \\ \mathbb{V}[I^{\text{tr}}] &\leq \frac{2b^2 B_A^2 C_{\epsilon, d_1}^2}{N^{2-2\epsilon-2\max_i A_i}} + \frac{2\mathbb{E}[|\bar{g}_h|^2 |f'(\bar{g}_h)|^2] \tilde{L}^2(c(\text{TOL}))^2 C_{\epsilon, d_2}^2}{NM^{2-2\epsilon}} \\ &\quad + \frac{\mathbb{E}[|\bar{g}_h|^4 |f''(K(\text{TOL})\bar{g}_h)|^2] (\Gamma_{d_1} + 1) \tilde{L}^4(c(\text{TOL}))^4 C_{\epsilon, d_2}^4}{2NM^{4-4\epsilon}}, \end{aligned}$$

for a specified error tolerance $\text{TOL} > 0$, where I^{tr} is the truncated integral introduced in (148) with $c(\text{TOL})$ as in (149). Moreover, this result holds for any $\epsilon > 0$, and $0 < K(\text{TOL}) < 2$, where $C_{\epsilon, d_1}, C_{\epsilon, d_2} \rightarrow \infty$ as $\epsilon \rightarrow 0$, $B_A \rightarrow \infty$ as $\min_i A_i \rightarrow 0$, and $\Gamma_{d_1} \rightarrow \infty$ as $d_1 \rightarrow \infty$.

Proof. The result follows directly from Proposition 3, Proposition 4, Lemma 2, and Lemma 3. For the logarithm, it follows that $|f'(\bar{g})| = |\bar{g}^{-1}|$, $|f''(\bar{g})| = |\bar{g}^{-2}|$, and $|f'''(\bar{g})| = |2\bar{g}^{-3}|$ and thus the terms on the right-hand sides of (167) and (168) are bounded. From the introduction of K in (50), it immediately follows that the condition $0 < K(\text{TOL}) < 2$ is equivalent to

$$(169) \quad C_{\epsilon, d_2} M^{-1+\epsilon} \tilde{L}c(\text{TOL}) < 1,$$

which is verified for $M = \mathcal{O}\left(\log(\text{TOL}^{-1})^{\frac{1}{2(1-\epsilon)}}\right)$, imposing a weaker requirement than the condition in (77). \square

Remark 13 (Total complexity of the EIG estimation via the rDLQMC estimator). *The total computational complexity to estimate the EIG for a prescribed tolerance (TOL) via the rDLQMC estimator differs from the result stated in Proposition 5 by a log factor introduced by the restriction to truncated observation noise. This immediately follows from Proposition 5 for the error bounds presented in Corollary 1.*

APPENDIX G. DERIVATION OF THE FINITE ELEMENT FORMULATION

We let $(\Omega, \mathcal{F}, \mathbb{P})$ be a complete probability space with outcomes Ω , σ -field \mathcal{F} , and probability measure \mathbb{P} . Moreover, $\mathcal{H} := H^1(\mathcal{D}) \oplus H^1(\mathcal{D})$ is defined as the space of the solution for the coupled thermomechanical fields $(\vartheta(\omega), \mathbf{u}(\omega))$ for $\omega \in \Omega$, where $H^1(\mathcal{D})$ represents the standard Sobolev space $W^{1,2}(\mathcal{D})$ with its corresponding Sobolev norm. Furthermore, the Bochner space is defined as follows:

$$(170) \quad V_\vartheta \oplus V_U \equiv L_{\mathbb{P}}^2(\Omega; \mathcal{H}) := \left\{ (\vartheta, \mathbf{u}) : \Omega \rightarrow \mathcal{H} \quad \text{s.t.} \quad \left(\int_{\Omega} \|(\vartheta(\omega), \mathbf{u}(\omega))\|_{\mathcal{H}}^2 d\mathbb{P}(\omega) \right)^{1/2} < \infty \right\}.$$

We aimed to determine $(\vartheta, \mathbf{u}) \in L_{\mathbb{P}}^2(\Omega; \mathcal{H})$ such that the weak formulations, (111) and (115), are fulfilled for all $(\hat{\vartheta}, \hat{\mathbf{u}}) \in L_{\mathbb{P}}^2(\Omega; \mathcal{H})$.

REFERENCES

- [1] Ryan KJ. Estimating expected information gains for experimental designs with application to the random fatigue-limit model. *Journal of Computational and Graphical Statistics*, 12:585–603, 2003.
- [2] Beck J, Dia BM, Espath LF, Long Q, and Tempone R. Fast Bayesian experimental design: Laplace-based importance sampling for the expected information gain. *Computer Methods in Applied Mechanics and Engineering*, 334:523–553, 2018.
- [3] Beck J, Dia BM, Espath LF, and Tempone R. Multilevel double loop Monte Carlo and stochastic collocation methods with importance sampling for Bayesian optimal experimental design. *International Journal for Numerical Methods in Engineering*, 121:3482–3503, 2020.
- [4] Carlon AG, Dia BM, Espath LF, Lopez RH, and Tempone R. Nesterov-aided stochastic gradient methods using Laplace approximation for Bayesian design optimization. *Computer Methods in Applied Mechanics and Engineering*, 363:112909, 2020.
- [5] Shannon CE. A mathematical theory of communication. *Bell System Technical Journal*, 27:379–423, 1948.
- [6] Kullback S. *Information theory and statistics*. Wiley, 1959.

- [7] Long Q, Scavino M, Tempone R, and Wang S. Fast estimation of expected information gains for Bayesian experimental designs based on Laplace approximations. *Computer Methods in Applied Mechanics and Engineering*, 259:24–39, 2013.
- [8] Long Q. Multimodal information gain in Bayesian design of experiments. *arXiv preprint arXiv:2108.07224*, 2021.
- [9] Schillings C, Sprungk B, and Wacker P. On the convergence of the Laplace approximation and noise-level-robustness of Laplace-based Monte Carlo methods for Bayesian inverse problems. *Numerische Mathematik*, 145:915–971, 2020.
- [10] Wacker P. Laplace’s method in Bayesian inverse problems. *arXiv preprint arXiv:1701.07989*, 2017.
- [11] Chaloner K and Verdinelli I. Bayesian experimental design: a review. *Statistical Sciences*, 10:273–304, 1995.
- [12] Kullback S and Leibler RA. On information and sufficiency. *Annals of Mathematical Statistics*, 22:79–86, 1951.
- [13] Stigler SM. Laplace’s 1774 memoir on inverse probability. *Statistical Science*, 1:359–378, 1986.
- [14] Lindley DV. On a measure of information provided by an experiment. *Annals of Mathematical Statistics*, 27:986–1005, 1956.
- [15] Tierney L and Kadane JB. Accurate approximations for posterior moments and marginal densities. *Journal of the American Statistical Association*, 81:82–86, 1986.
- [16] Tierney L, Kass RE, and Kadane JB. Fully exponential Laplace approximations to expectations and variances of nonpositive functions. *Journal of the American Statistical Association*, 84:710–716, 1989.
- [17] Kass RE, Tierney L, and Kadane JB. The validity of posterior expansions based on Laplace’s method. in: *Geisser S, Hodges JS, Press SJ, and Zellner A (Eds.), Essays in Honor of George Barnard*, 473–488, 1990.
- [18] Long Q, Scavino M, Tempone R, and Wang S. A Laplace method for under-determined Bayesian optimal experimental designs. *Computer Methods in Applied Mechanics and Engineering*, 285:849–876, 2015.
- [19] Giles MB. Multilevel Monte Carlo path simulation. *Operations Research*, 56(3):607–617, 2008.
- [20] Tsilifis P, Ghanem RG, and Hajali P. Efficient Bayesian experimentation using an expected information gain lower bound. *SIAM/ASA Journal on Uncertainty Quantification*, 5:30–62, 2017.
- [21] Goda T, Daisuke M, Kei T, and Kozo S. Decision-theoretic sensitivity analysis for reservoir development under uncertainty using multilevel quasi-Monte Carlo methods. *Computational Geosciences*, 22:1009–1020, 2018.
- [22] Xu Z, He Z, and Wang X. Efficient risk estimation via nested multilevel quasi-Monte Carlo simulation. *Journal of Computational and Applied Mathematics*, 443:115745, 2024.
- [23] Fang W, Wang Z, Giles MB, Jackson CH, Welton NJ, Andrieu C, and Thom H. Multilevel and quasi Monte Carlo methods for the calculation of the expected value of partial perfect information. *Medical Decision Making*, 42(2):168–181, 2022.
- [24] Cafilisch RE. Monte Carlo and quasi-Monte Carlo methods. *Acta Numerica*, 1–49, 1998.
- [25] Hickernell FJ. Lattice rules: How well do they measure up? In: *Hellekalek P and Larcher G (Eds.). Random and Quasi-Random Point Sets. Lecture Notes in Statistics 138*, New York, Springer, 109–166, 1998.
- [26] Niederreiter H. Random number generation and quasi-Monte Carlo methods. *SIAM*, Philadelphia, 1992.
- [27] Owen AB. Quasi-Monte Carlo sampling. In: *Monte Carlo Ray Tracing: SIGGRAPH*, 69–88, 2003.
- [28] Tuffin B. Randomization of quasi-Monte Carlo methods for error estimation: survey and normal approximation. In: *Monte Carlo Methods and Applications*, De Gruyter, 10(3-4):617–628, 2004.
- [29] Durrett R. Probability: Theory and examples. *Cambridge University Press*, 2019.
- [30] Dick J and Pillichshammer F. Digital nets and sequences: discrepancy theory and quasi-Monte Carlo integration. *Cambridge University Press*, 2010.
- [31] Dick J, Kuo FY, and Sloan IH. High-dimensional integration: the quasi-Monte Carlo way. *Acta Numerica*, 133–288, 2013.
- [32] Sobol’ IM. Distribution of points in a cube and approximate evaluation of integrals. *Ž. Vyčisl. Mat. i Mat. Fiz. (in Russian)*, 7:784–802, 1967.
- [33] Drovandi CC and Tran M-N. Improving the efficiency of fully Bayesian optimal design of experiments using randomised Quasi-Monte Carlo. *Bayesian Analysis*, 13(1):139–162, 2018.
- [34] L’Ecuyer P, Munger D, and Tuffin B. On the distribution of integration error by randomly-shifted lattice rules. *Electronic Journal of Statistics*, 4:950–993, 2010.
- [35] Gobet E, Lerasle M, and Métivier D. Mean estimation for randomized Quasi Monte Carlo method. *Hal preprint hal-03631879v2*, 2022.
- [36] Helin T and Kretschmann R. Non-asymptotic error estimates for the Laplace approximation in Bayesian inverse problems. *Numerische Mathematik*, 150:521–549, 2022.
- [37] L’Ecuyer P. Randomized Quasi-Monte Carlo: An introduction for practitioners. In: *Owen A and Glynn P (Eds.). Monte Carlo and Quasi-Monte Carlo Methods. MCQMC 2016. Springer Proceedings in Mathematics & Statistics*, Cham, Springer 241:29–52, 2018.
- [38] Hlawka E. Funktionen von beschränkter Variation in der Theorie der Gleichverteilung. *Annali di Matematica Pura ed Applicata*, 54:325–333, 1961.
- [39] Owen AB. Local antithetic sampling with scrambled nets. *The Annals of Statistics*, 36(5):2319–2343, 2008.
- [40] Farhat C, Park KC, and Dubois-Pelerin Y. An unconditionally stable staggered algorithm for transient finite element analysis of coupled thermoelastic problems. *Computer Methods in Applied Mechanics and Engineering*, 85(3):349–365, 1991.
- [41] Haji-Ali A-L, Nobile F, Tamellini, L, and Tempone R. Multi-index stochastic collocation convergence rates for random PDEs with parametric regularity. *Foundations of Computational Mathematics*, 16:1555–1605, 2016.
- [42] Owen AB. Halton sequences avoid the origin. *SIAM Review*, 48:487–503, 2006.
- [43] Liu Y and Tempone R. Nonasymptotic convergence rate of quasi-Monte Carlo: applications to linear elliptic PDEs with lognormal coefficients and importance samplings. *arXiv preprint arXiv:2310.14351*, 2023.
- [44] Graham IG, Kuo FY, Nichols JA, Scheichl R, Schwab C, and Sloan IH. Quasi-Monte Carlo finite element methods for elliptic PDEs with lognormal random coefficients. *Numerische Mathematik*, 131:329–368, 2015.

- [45] He Z, Zheng Z, and Wang X. On the error rate of importance sampling with randomized quasi-Monte Carlo. *SIAM Journal on Numerical Analysis*, 61(2):10.1137/22M1510121, 2023.
- [46] Ouyang D, Wang X, and He Z. Quasi-Monte Carlo for unbounded integrands with importance sampling. *arXiv preprint arXiv:2310.00650*, 2023.
- [47] Owen AB. Randomly permuted (t,m,s)-nets and (t,s)-sequences. in: *Niederreiter H and Shiue PJS (Eds.), Monte Carlo and Quasi-Monte Carlo methods in Scientific Computing. Lecture Notes in Statistics 106*, New York, Springer, 1995.
- [48] Rainforth T, Cornish R, Yang H, Warrington A, and Wood F. On nesting Monte Carlo estimators. *Proceedings of the 35th International Conference on Machine Learning, PLMR 80* Stockholm, 2008.
- [49] Hong LJ, and Juneja S. Estimating the mean of a non-linear function of conditional expectation. in: *Rossetti MD, Hill RR, Johansson B, Dunkin A and Ingalls RG (Eds.), Proceedings of the 2009 Winter Simulation Conference (WSC)* Austin, 1223–1236, 2009.
- [50] L’Ecuyer P, Nakayama MK, Owen AB, and Tuffin B. Confidence intervals for randomized quasi-Monte Carlo estimators. *Winter Simulation Conference, San Antonio, US*, 2023.
- [51] Fort G, Gobet E, and Moulines E. MCMC design-based non-parametric regression for rare event. Application to nested risk computations. *Monte Carlo Methods and Applications*, 23(1):21–42, 2017.
- [52] Foster A, Jankowiak M, Bingham E, Horsfall P, Teh YW, Rainforth T, and Goodman N. Variational Bayesian optimal experimental design. *Advances in Neural Information Processing Systems 32*, 2019.
- [53] Goda T, Hironaka T, and Iwamoto T. Multilevel Monte Carlo estimation of expected information gains. *Stochastic Analysis and Applications*, 38(4):581–600, 2020.
- [54] Goda T, Hironaka T, Kitade W, and Foster A. Unbiased MLMC stochastic gradient-based optimization of Bayesian experimental designs. *SIAM Journal on Scientific Computing*, 44(1):A286–A311, 2022.
- [55] Kuo FY, Schwab C, and Sloan IH. Quasi-Monte Carlo finite element methods for a class of elliptic partial differential equations with random coefficients. *SIAM Journal on Numerical Analysis*, 50(6):3351–3374, 2012.
- [56] Kuo FY, Schwab C, and Sloan IH. Multi-level quasi-Monte Carlo finite element methods for a class of elliptic PDEs with random coefficients. *Foundations of Computational Mathematics*, 15:411–449, 2015.
- [57] Ryan EG, Drovandi CC, Thompson MH and Pettitt AN. Towards Bayesian experimental design for nonlinear models that require a large number of sampling times. *Computational Statistics and Data Analysis*, 70:45–60, 2014.
- [58] Owen AB. Scrambled net variance for integrals of smooth functions. *The Annals of Statistics*, 25:1541–1562, 1997.
- [59] Cranley R, and Patterson TNL. Randomization of number theoretic methods for multiple integration. *SIAM Journal on Numerical Analysis*, 13(6):904–914, 1976.
- [60] Pan Z, and Owen AB. The nonzero gain coefficients of Sobol’s sequences are always powers of two. *Journal of Complexity*, 75:101700, 2023.
- [61] Bornkamp B. Approximating probability densities by iterated Laplace approximations. *Journal of Computational and Graphical Statistics*, 20(3):656–669, 2011.
- [62] Bisetti F, Kim D, Knio O, Long Q, and Tempone R. Optimal Bayesian experimental design for priors of compact support with application to shock-tube experiments for combustion kinetics. *International Journal for Numerical Methods in Engineering*, 108:136–155, 2016.
- [63] Kaarnioja V, and Schillings C. Quasi-Monte Carlo for Bayesian design of experiment problems governed by parametric PDEs. *arXiv preprint arXiv:2405.03529 [v2]*, 2024.
- [64] Long Q. Multimodal information gain in Bayesian design of experiments. *Computational Statistics*, 37(2):865–885 2022.
- [65] Patel JK, and Read CB. Handbook of the normal distribution. *2nd ed.*, New York, Marcel Dekker, 1996.